Contribution from the Department of Chemistry,
University of Houston, University Park, Houston, Texas 77004

# Structures and Mechanism of Multiple Ligand Substitutions in Bicapped Tetracobalt Clusters

M. G. Richmond and J. K. Kochi*

*Received October 18, 1985*

The planar tetracobalt carbonyl cluster with a pair of $\mu_4$-phosphinidene caps $Co_4(CO)_{10}(\mu_4\text{-}PPh)_2$ undergoes ready ligand substitution with trimethyl phosphite thermally to afford the mono, bis, tris, and tetrakis derivatives. The molecular structures of the substitution products by X-ray crystallography establish the stepwise introduction of phosphites at separate cobalt centers. Electronic and steric effects play important roles in the sequential introduction and the stereochemical disposition of the phosphite ligands in the bis-, tris-, and tetrakis-substitution products. The kinetics and activation parameters indicate that the mono- and bis-substitutions occur primarily via an associative mechanism, whereas a dissociative process is dominant in the tris- and tetrakis-substitutions. The fluxional behavior of the carbonyl ligands, as observed by the temperature-dependent $^{13}C$ NMR spectra, is in accord with the extensive stereomutation of ligands during substitution—particularly in those steps leading to the tris and tetrakis derivatives. The changeover in the mechanism of ligand substitution with the extent of phosphite substitution of the tetracobalt cluster is discussed.

## Introduction

Polynuclear metal clusters remain under active investigation as potential catalysts for the utilization of carbon monoxide in olefin hydroformylation and reduction, as well as for the Fischer–Tropsch and related reactions.[1-4] Interest stems from the possibility extant in clusters for cooperative metal interactions leading to multisite activation of the substrates.[5-9] Polynuclear clusters also offer ready access to multiple redox levels which are promoted by the presence of contiguous metal centers.[10] The latter has led to the discovery of facile and selective ligand as well as metal substitutions in a variety of clusters through the participation of electron-transfer chain or ETC catalysis.[11-14] Indeed

**Table I.** Infrared Spectra in the $\nu_{CO}$ Region of the Tetracobalt Clusters $Co_4(CO)_{10-n}[P(OMe)_3]_n(PPh)_2$[a]

| tetracobalt cluster | IR band, $cm^{-1}$ |
|---|---|
| $Co_4(CO)_{10}(PPh)_2$ | 2040.8 (vs), 2029.1 (s), 2015.4 (s), 1870.9 (m) |
| $Co_4(CO)_9[P(OMe)_3](PPh)_2$ | 2058.4 (m), 2023.2 (vs), 2007.6 (s), 1850.4 (m) |
| $Co_4(CO)_8[P(OMe)_3]_2(PPh)_2$ | 2038.9 (m), 2007.6 (vs), 1985.1 (s), 1834.8 (m) |
| $Co_4(CO)_7[P(OMe)_3]_3(PPh)_2$ | 2015.4 (s), 1971.5 (vs, br), 1813.3 (m) |
| $Co_4(CO)_6[P(OMe)_3]_4(PPh)_2$ | 1985.1 (m), 1955.1 (s, br), 1795.7 (m) |

[a] All spectra measured in $CH_2Cl_2$ solvent to within $\pm 2$ $cm^{-1}$.

(1) (a) Bricker, J. C.; Nagel, C. C.; Bhattachargya, A. A.; Shore, S. G. *J. Am. Chem. Soc.* **1985**, *107*, 377. (b) Bricker, J. C.; Nagel, C. C.; Shore, S. G. *J. Am. Chem. Soc.* **1982**, *104*, 1444. (c) Ford, P. C. *Acc. Chem. Res.* **1981**, *14*, 31. (d) Yarrow, P.; Cohen, H.; Ungermann, C.; Vandenberg, D.; Ford, P. C.; Rinker, R. G. *J. Mol. Catal.* **1983**, *22*, 239. (e) Ford, P. C.; Vandenberg, D. M.; Suzuki, T. M. *J. Organomet. Chem.* **1984**, *272*, 309. (f) Gross, D. C.; Ford, P. C. *J. Am. Chem. Soc.* **1985**, *107*, 585.

(2) (a) Keister, J. B.; Shapley, J. R. *J. Am. Chem. Soc.* **1976**, *98*, 1056. (b) Doi, Y.; Koshizuka, K.; Keii, T. *Inorg. Chem.* **1982**, *21*, 2732. (c) Cho, B. R.; Laine, R. M. *J. Mol. Catal.* **1982**, *15*, 383. (d) Mani, D.; Vahrenkamp, H. *J. Mol. Catal.* **1985**, *29*, 305.

(3) (a) Kang, H. C.; Mauldin, C. H.; Cole, T.; Slegeir, W.; Cann, K.; Pettit, R. *J. Am. Chem. Soc.* **1977**, *99*, 8323. (b) Laine, R. M. *Ann. N.Y. Acad. Sci.* **1980**, *33*, 124. (c) Ryan, R. C.; Pittman, C. U.; O'Connor, J. P. *J. Am. Chem. Soc.* **1977**, *99*, 1986. (d) Richmond, M. G.; Absi-Halabi, M.; Pittman, C. U. *J. Mol. Catal.* **1984**, *22*, 367. (e) Pittman, C. U.; Richmond, M. G.; Wilemon, G. M.; Absi-Halabi, M. In *Catalysis of Organic Reactions*; Kosak, J. R., Ed.; Marcel Dekker: New York, 1984; Chapter 5.

(4) (a) Dombek, B. D. *J. Am. Chem. Soc.* **1980**, *102*, 6855. (b) Knifton, J. K. *J. Am. Chem. Soc.* **1981**, *103*, 3959. (c) Cole, T.; Ramage, R.; Cann, K.; Pettit, R. *J. Am. Chem. Soc.* **1980**, *102*, 6184. (d) Masters, C. *Adv. Organomet. Chem.* **1979**, *17*, 61.

(5) (a) Muetterties, E. L. *Science (Washington, D.C.)* **1977**, *196*, 839. (b) Robinson, A. L. *Science (Washington, D.C.)* **1976**, *194*, 1150. (c) Pittman, C. U.; Ryan, R. C. *CHEMTECH* **1978**, 170. (d) Muetterties, E. L. *Bull. Soc. Chim. Belg.* **1975**, *84*, 959. (e) Muetterties, E. L. *Bull. Soc. Chim. Belg.* **1976**, *85*, 451. (f) Muetterties, E. L.; Rhodin, T. N.; Band, E.; Brucker, C. F.; Pretzer, W. R. *Chem. Rev.* **1979**, *79*, 91.

(6) (a) Roland, E.; Vahrenkamp, H. *J. Mol. Catal.* **1983**, *21*, 233. (b) Bernhardt, W.; Vahrenkamp, H. *Angew. Chem., Int. Ed. Engl.* **1984**, *23*, 141. (c) Bernhardt, W.; Vahrenkamp, H. *Angew. Chem., Int. Ed. Engl.* **1984**, *23*, 381.

(7) (a) Andrews, M. A.; Kaesz, H. D. *J. Am. Chem. Soc.* **1979**, *101*, 7238, 7255. (b) Szostak, R.; Strouse, C. E.; Kaesz, H. D. *J. Organomet. Chem.* **1980**, *191*, 243. (c) Lin, Y. C.; Knobler, C. B.; Kaesz, H. D. *J. Am. Chem. Soc.* **1981**, *103*, 1981. (d) Kaesz, H. D.; Knobler, C. B.; Andrews, M. A.; Van Buskirk, G.; Szostak, R.; Strouse, C. E.; Lin, Y. C.; Mayr, A. *Pure Appl. Chem.* **1982**, *54*, 131.

(8) (a) Laine, R. M.; Thomas, D. W.; Cary, L. W.; Buttrill, S. E. *J. Am. Chem. Soc.* **1978**, *100*, 6527. (b) Shvo, Y.; Laine, R. M. *J. Chem. Soc., Chem. Commun.* **1980**, *753*. (c) Shvo, Y.; Thomas, D. W.; Laine, R. M. *J. Am. Chem. Soc.* **1981**, *103*, 2461.

(9) (a) Sinfelt, J. H. *Catal. Rev.—Sci. Eng.* **1974**, *9*, 147. (b) Ugo, R. *Catal. Rev.—Sci. Eng.* **1975**, *11*, 225. (c) Lewis, J.; Johnson, B. F. G. *Pure Appl. Chem.* **1975**, *44*, 43. (d) Muetterties, E. L. *Pure Appl. Chem.* **1978**, *50*, 941. (e) Smith, A. K.; Basset, J. M. *J. Mol. Catal.* **1977**, *2*, 229. (f) Muetterties, E. L.; Krause, M. J. *Angew. Chem., Int. Ed. Engl.* **1983**, *22*, 135.

(10) (a) Ferguson, J. A.; Meyer, T. J. *J. Am. Chem. Soc.* **1972**, *94*, 3409. (b) Toan, T.; Teo, B. K.; Ferguson, J. A.; Meyer, T. J.; Dahl, L. F. *J. Am. Chem. Soc.* **1977**, *99*, 408. (c) Madach, T.; Vahrenkamp, H. *Chem. Ber.* **1981**, *114*, 505. (d) Lemoine, P. *Coord. Chem. Rev.* **1982**, *47*, 55. (e) Pickett, C. J. *J. Chem. Soc., Chem. Commun.* **1985**, 323.

(11) For some examples of electron-induced ligand substitution and metal exchange reactions, see: (a) Bezems, G. T.; Rieger, P. H.; Visco, S. *J. Chem. Soc., Chem. Commun.* **1981**, 265. (b) Darchen, A.; Mahe, C.; Patin, H. *J. Chem. Soc., Chem. Commun.* **1982**, 243. (c) Jensen, S.; Robinson, B. H.; Simpson, J. J. *Chem. Soc., Chem. Commun.* **1983**, 1081. (d) Arewgoda, C. M.; Robinson, B. H.; Simpson, J. *J. Chem. Soc., Chem. Commun.* **1982**, 284. (e) Darchen, A.; Lhadi, E. L.; Patin, H. *J. Organomet. Chem.* **1983**, *259*, 189. (f) Darchen, A.; Mahe, C.; Patin, H. *Nouv. J. Chim.* **1982**, *6*, 539. (g) Bruce, M. I.; Hambley, T. W.; Nicholson, B. K.; Snow, M. R. *J. Organomet. Chem.* **1982**, *235*, 83. (h) Bruce, M. I.; Kehoe, D. C.; Matisons, J. G.; Nicholson, B. K.; Rieger, P. H.; Williams, M. L. *J. Chem. Soc., Chem. Commun.* **1982**, 442. (i) Venalainen, T.; Pakkanen, T. *J. Organomet. Chem.* **1984**, *266*, 269. (j) Honrath, U.; Vahrenkamp, H. *Z. Naturforsch., B: Anorg. Chem. Org. Chem.* **1984**, *39B*, 559.

(12) For a general discussion of the ETC reaction and catalytic implications, see: (a) Chanon, M.; Tobe, M. L. *Angew. Chem., Int. Ed. Engl.* **1982**, *21*, 1. (b) Bunnett, J. F. *Acc. Chem. Res.* **1978**, *11*, 413. (c) Saveant, J. M. *Acc. Chem. Res.* **1980**, *13*, 323.

(13) For orbital considerations, see: (a) Beurich, H.; Madach, T.; Richter, F.; Vahrenkamp, H. *Angew. Chem., Int. Ed. Engl.* **1979**, *18*, 690. (b) Honrath, U.; Vahrenkamp, H. *Z. Naturforsch., B: Anorg. Chem., Org. Chem.* **1984**, *39B*, 545. (c) Sowa, T.; Kawamura, T.; Yonezawa, T. *J. Organomet. Chem.* **1985**, *284*, 337. (d) Matheson, T. W.; Peake, B. M.; Robinson, B. H.; Simpson, J.; Watson, D. J. *J. Chem. Soc., Chem. Commun.* **1973**, 894. (e) Peake, B. M.; Robinson, B. H.; Simpson, J.; Watson, D. J. *Inorg. Chem.* **1977**, *16*, 405. (f) Peake, B. M.; Rieger, P. H.; Robinson, B. H.; Simpson, J. *Inorg. Chem.* **1979**, *18*, 1000. (g) Peake, B. M.; Rieger, P. H.; Robinson, B. H.; Simpson, J. *Inorg. Chem.* **1981**, *20*, 2540. (h) Casagrande, L. S.; Chen, T.; Rieger, P. H.; Robinson, B. H.; Simpson, J.; Visco, S. J. *Inorg. Chem.* **1984**, *23*, 2019. (i) Arewgoda, C. M.; Bond, A. M.; Dickson, R. S.; Mann, T. F.; Moir, J. E.; Rieger, P. H.; Robinson, B. H.; Simpson, J. *Organometallics* **1985**, *4*, 1077.

0020-1669/86/1325-1334$01.50/0 

our initial interest in polynuclear carbonyls stems from the observation of an efficient ETC catalysis of the tetracobalt cluster $Co_4(CO)_{10}(\mu_4\text{-}PPh)_2$ (I).[15,16] This polynuclear metal carbonyl

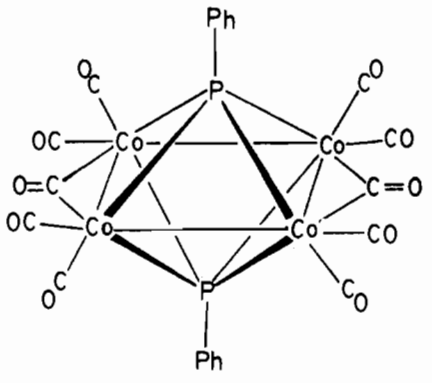

I

merits special attention since it represents one of the rare examples in which the intact cluster can apparently function as the active catalyst in the hydroformylation of olefins.[17] In particular only limited information exists for the multiple substitution of the carbonyl ligands and the stereodynamic behavior of the metal–metal bonds and the ancillary ligands, as well as the chemical reactivity of such a catalytically viable cluster polyhedron. Accordingly, we have focused our attention in this study on the regiochemistry and mechanism of multiple ligand substitution of the tetracobalt cluster I. We began with trimethyl phosphite as the nucleophile, i.e.

$$\underset{\text{I}}{Co_4(CO)_{10}(\mu_4\text{-}PPh)_2} + nP(OMe)_3 \rightarrow \underset{\text{II–V}}{Co_4(CO)_{10-n}[P(OMe)_3]_n(\mu_4\text{-}PPh)_2} \quad (1)$$

since the mono- and bis(phosphite) derivatives II and III with $n$ = 1 and 2, respectively, have already been prepared.[18] The substitution pattern in this cluster is established by the X-ray crystallographic determination of the bis-, tris-, and tetrakis(phosphite) derivatives. The kinetics of the stepwise replacement of four carbonyl ligands in eq 1 to form the phosphite-substituted clusters II–V provide insight into the involvement of the metal–metal bond in the activation of this polynuclear cluster.

## Results

**I. Ligand Substitution of the Tetracobalt Cluster I by Trimethyl Phosphite.** The ligand substitutions of the tetracobalt clusters with trimethyl phosphite were carried out thermally in either benzene or toluene solutions by serially replacing a single carbonyl ligand in the parent carbonyl I, the mono(phosphite) derivative II ($n$ = 1), the bis(phosphite) derivative III ($n$ = 2) and the tris(phosphite) derivative IV ($n$ = 3), as described in the Experimental Section. The preparations of the phosphite-substituted clusters II–IV are also achieved in moderate to near-quantitative yields by simply adding a stoichiometric measure of trimethyl phosphite to I all at once and then controlling the reaction temperature. Optimum conditions for maximum conversion to the desired derivative were ascertained by monitoring the appearance of each product by its characteristic infrared spectrum (vide infra) or by thin-layer chromatography. The tetrakis-substituted cluster V ($n$ = 4) was readily obtained in high yield by heating the parent cluster in the presence of excess trimethyl phosphite. At no time could we observe any discrete products of further substitution (i.e., eq 1 with $n \geq 5$) or fragmentation of the cluster framework.[19-24]

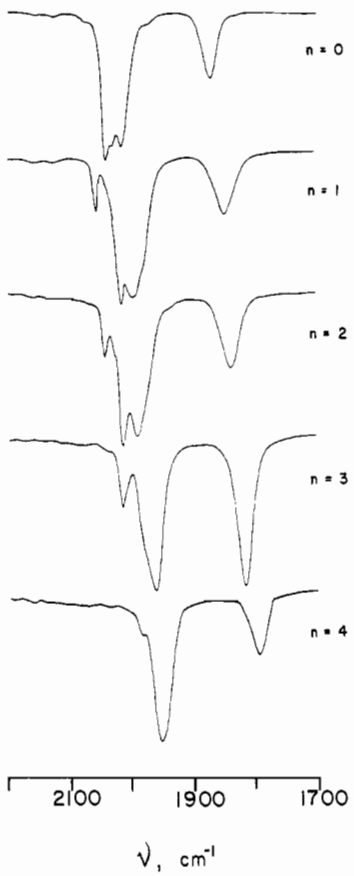


**Figure 1.** Infrared bands for $\nu_{CO}$(stretch) of the tetracobalt derivatives $Co_4(CO)_{10-n}[P(OMe)_3]_n(\mu_4\text{-}PPh)_2$.

**Table II.** X-ray Crystallographic Data for the Tetracobalt Clusters

| | $Co_4(CO)_8[P(OMe)_3]_2(PPh)_2$ | $Co_4(CO)_6[P(OMe)_3]_4(PPh)_2$ |
|---|---|---|
| space group | $P2_1/n$, monoclinic | $P\bar{1}$, triclinic |
| cell constants | | |
| $a$, Å | 12.863 (1) | 11.645 (2) |
| $b$, Å | 10.111 (6) | 11.767 (1) |
| $c$, Å | 13.854 (2) | 17.836 (2) |
| $\alpha$, deg | | 92.13 (1) |
| $\beta$, deg | 96.88 (1) | 90.59 (1) |
| $\gamma$, deg | | 114.70 (1) |
| vol ($V$), Å$^3$ | 1789 | 2217.8 |
| molecular formula | $C_{26}H_{28}Co_4P_4O_{14}$ | $C_{30}H_{46}Co_4P_6O_{18}$ |
| fw | 924.14 | 1116.3 |
| formula units/cell ($Z$) | 2 | 2 |
| density ($\rho$), g cm$^{-3}$ | 1.72 | 1.67 |
| abs coeff ($\mu$), cm$^{-1}$ | 20.57 | 17.5 |
| radiation ($\lambda$, Å) | Mo K$\alpha$ (0.71073) | Mo K$\alpha$ (0.71073) |
| collection range, deg | $4 < 2\theta < 40$ | $4 < 2\theta < 35$ |
| scan width ($\Delta\theta$), deg | (1.00 + 0.35 tan $\theta$) | (0.90 + 0.35 tan $\theta$) |
| max scan time, s | 180 | 200 |
| scan speed range, deg min$^{-1}$ | 0.5–5.0 | 0.40–5.00 |
| total data collected | 1896 | 2710 |
| independent data | 1276 | 1981 |
| total variables | 220 | 523 |
| $R = \sum\|\|F_o\| - \|F_c\|\|/\sum\|F_o\|$ | 0.023 | 0.029 |
| $R_w = [\sum w(\|F_o\| - \|F_c\|)^2/\sum w\|F_o\|^2]^{1/2}$ | 0.026 | 0.032 |
| weights | $w = \sigma(F)^{-2}$ | $w = 1.0$ |

The infrared spectra in the carbonyl region (2200–1700 cm$^{-1}$) of the parent cluster I and each of the phosphite derivatives (II–V)

(14) For effect on catalytic activity see: (a) Penfold, B. R.; Robinson, B. H. *Acc. Chem. Res.* **1973**, *6*, 73. (b) Vahrenkamp, H. *Struct. Bonding (Berlin)* **1977**, *32*, 1.
(15) Richmond, M. G.; Kochi, J. K. *Inorg. Chem.* **1986**, *25*, 656.
(16) Ryan, R. C.; Dahl, L. F. *J. Am. Chem. Soc.* **1975**, *97*, 6904.
(17) Pittman, C. U.; Wilemon, G. M.; Wilson, W. D.; Ryan, R. C. *Angew. Chem., Int. Ed. Engl.* **1980**, *19*, 478.
(18) (a) Kouba, J. K.; Pierce, J. L.; Walton, R. A. *J. Organomet. Chem.* **1980**, *202*, C105. (b) Kouba, J. K.; Muetterties, E. L.; Thompson, M. R.; Day, V. W. *Organometallics* **1983**, *2*, 1065.
(19) Cf.: (a) Huttner, G. *Nachr. Chem., Tech. Lab.* **1979**, *27*, 261. (b) Deeming, A. J. In *Transition Metal Clusters*; Johnson, B. F. G., Ed.; Wiley: New York, 1980; Chapter 6. (c) Vahrenkamp, H. *Angew. Chem., Int. Ed. Engl.* **1978**, *17*, 379.
(20) See also: Chini, P.; Heaton, B. T. *Top. Curr. Chem.* **1977**, *71*, 1.

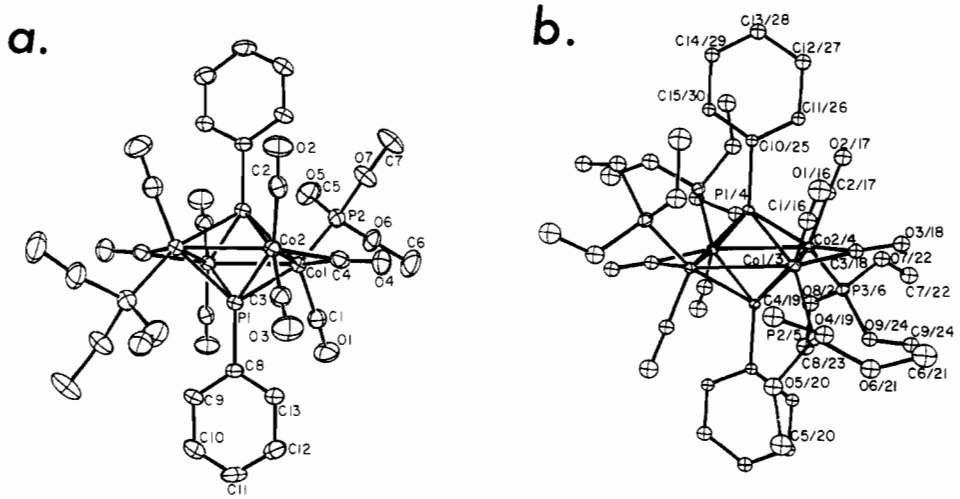


**Figure 2.** ORTEP diagram of (a) the bis-substitution product $Co_4(CO)_8[P(OMe)_3]_2(\mu_4\text{-}PPh)_2$ (III) showing the 1,3-syn/anti stereochemistry of the phosphite ligands and (b) the tetrakis-substitution product $Co_4(CO)_6[P(OMe)_3]_4(\mu_4\text{-}PPh)_2$ (V) showing 1,2,3,4-placement of phosphite ligands with syn/syn/anti/anti stereochemistry. For clarity, the hydrogen atoms are not included.

are illustrated in Figure 1. The consistent trend within this family of homologues emphasizes that the stretching bands associated with both the terminal and bridging ligands are systematically shifted to lower energies by successive phosphite substitution (Table I). This observation is consistent with a greater degree of $\pi$ back-bonding in the cobalt-carbon linkages with increasing substitution owing to the presence of the phosphite, which is a stronger $\sigma$-donor but weaker $\pi$-acceptor ligand than the displaced carbon monoxide.[25]

**II. Molecular Structures of the Trimethyl Phosphite Derivatives by X-ray Crystallography.** Single crystals of the bis(phosphite), tris(phosphite), and tetrakis(phosphite) derivatives III, IV, and V (i.e., $n$ = 2, 3, 4) were successfully grown, and the X-ray crystallographic data for the bis- and tetrakis(phosphite) derivatives are summarized in Table II. The final fractional coordinates are listed in Tables III and IV. The molecular configuration and the numbering scheme of $Co_4(CO)_8[P(OMe)_3]_2(PPh)_2$ and $Co_4(CO)_6[P(OMe)_3]_4(PPh)_2$ are presented in the ORTEP diagrams in parts a and b of Figure 2, respectively. Owing to the unique crystallographic features of the tris(phosphite) derivative IV ($n$ = 3), the details of the X-ray structure will be presented separately.[26] In each case, the cluster consists of four cobalt atoms in a rectangular array whose shorter sides are bridged by $\mu$-carbonyl groups. The capping of the cobalt tetramer by a pair of $\mu_4$-phenylphosphinidene moieties completes the overall octahedral $Co_4P_2$ core common to all these clusters. Selected bond lengths and bond angles for $Co_4(CO)_8[P(OMe)_3]_2(PPh)_2$ and $Co_4(CO)_6[P(OMe)_3]_4(PPh)_2$ are presented in Tables V and VI, respectively.

**III. Kinetics of Ligand Substitution of the Tetracobalt Clusters by Trimethyl Phosphite.** The kinetics for the stepwise substitution of the tetracobalt cluster by trimethyl phosphite were measured in toluene solutions. The progress of each step of the ligand substitution could be easily followed by monitoring the absorbance decrease of the highest energy carbonyl band in the infrared spectrum of the reactant cluster.

**Table III.** Fractional Positional Parameters for the Non-Hydrogen Atoms of $Co_4(CO)_8[P(OMe)_3]_2(PPh)_2$[a]

| atom | $x$ | $y$ | $z$ | $B$, Å$^2$ |
|---|---|---|---|---|
| Co1 | 0.56647 (5) | 0.15805 (7) | 0.53484 (5) | 2.50 (1) |
| Co2 | 0.44438 (5) | 0.08725 (7) | 0.38758 (4) | 2.54 (1) |
| P1 | 0.4215 (1) | 0.0352 (1) | 0.54093 (9) | 2.45 (3) |
| P2 | 0.7302 (1) | 0.2116 (2) | 0.5386 (1) | 3.25 (3) |
| O1 | 0.5178 (3) | 0.3190 (4) | 0.6986 (3) | 5.8 (1) |
| O2 | 0.4893 (3) | 0.0221 (4) | 0.1914 (2) | 5.0 (1) |
| O3 | 0.2355 (3) | 0.1977 (4) | 0.3376 (3) | 5.6 (1) |
| O4 | 0.5126 (3) | 0.3660 (4) | 0.3922 (3) | 4.3 (1) |
| O5 | 0.8106 (3) | 0.1029 (4) | 0.5795 (3) | 5.1 (1) |
| O6 | 0.7729 (3) | 0.3327 (4) | 0.6059 (3) | 4.30 (9) |
| O7 | 0.7632 (3) | 0.2477 (4) | 0.4352 (3) | 4.9 (1) |
| C1 | 0.5362 (4) | 0.2585 (6) | 0.6323 (4) | 3.7 (1) |
| C2 | 0.4750 (4) | 0.0515 (5) | 0.2678 (4) | 3.2 (1) |
| C3 | 0.3167 (4) | 0.1536 (6) | 0.3588 (3) | 3.3 (1) |
| C4 | 0.5144 (4) | 0.2604 (5) | 0.4262 (3) | 3.2 (1) |
| C5 | 0.896 (1) | 0.108 (2) | 0.650 (1) | 4.0 (4)* |
| C5A | 0.914 (1) | 0.097 (2) | 0.611 (1) | 5.5 (4)* |
| C5B | 0.850 (1) | 0.094 (2) | 0.680 (1) | 4.8 (4)* |
| C6 | 0.7293 (5) | 0.4619 (6) | 0.5868 (5) | 6.7 (2) |
| C7 | 0.8698 (5) | 0.2814 (8) | 0.4187 (5) | 6.9 (2) |
| C8 | 0.3151 (4) | 0.0977 (5) | 0.6037 (3) | 2.6 (1) |
| C9 | 0.2714 (4) | 0.0178 (6) | 0.6701 (3) | 3.5 (1) |
| C10 | 0.1895 (4) | 0.0682 (6) | 0.7156 (4) | 4.6 (1) |
| C11 | 0.1541 (4) | 0.1930 (6) | 0.6968 (4) | 5.0 (2) |
| C12 | 0.1958 (4) | 0.2723 (6) | 0.6309 (4) | 4.7 (1) |
| C13 | 0.2778 (4) | 0.2230 (5) | 0.5849 (4) | 3.6 (1) |

[a] Estimated standard deviations in the least significant digit are included in parentheses. Atoms marked with an asterisk were refined isotropically.

**A. Monosubstitution** of the tetracobalt cluster was examined with $Co_4(CO)_{10}(PPh)_2$ and a measured excess of trimethyl phosphite, i.e.

$$\underset{\text{I}}{Co_4(CO)_{10}(PPh)_2} + P(OMe)_3 \rightarrow \underset{\text{II}}{Co_4(CO)_9[P(OMe)_3](PPh)_2} + CO \quad (2)$$

The changes in the infrared spectrum accompanying the ligand substitution of I in Figure 3 show the carbonyl bands of the product $Co_4(CO)_9[P(OMe)_3](PPh)_2$ (II) to appear and intensify at the expense of those of the reactant. Under the selected conditions given in Table VII, the competition from ligand substitution to the next higher homologue $Co_4(CO)_8[P(OMe)_3]_2(PPh)_2$ (III) was negligible—as typically shown by the clean infrared spectrum obtained finally (cf. Figure 3). The change in carbonyl absorbance follows first-order kinetics for at least 3 half-lives over the temperature range 15–42 °C. The plot of these pseudo-first-order rate constants ($k_{obsd}$) as a function of trimethyl phosphite con-

(21) For the effect of capping bridges on cluster stability, see: (a) Vahrenkamp, H.; Keller, E. *Chem. Ber.* **1979**, *109*, 229. (b) Langenbach, H. J.; Vahrenkamp, H. *Chem. Ber.* **1979**, *112*, 3390. (c) Langenbach, H. J.; Keller, E.; Vahrenkamp, H. *J. Organomet. Chem.* **1979**, *171*, 259.
(22) See also ref 23 and 24.
(23) (a) Schneider, J.; Zsolnai, L.; Huttner, G. *Chem. Ber.* **1982**, *115*, 989. (b) Schneider, J.; Zsolnai, L.; Huttner, G. *J. Organomet. Chem.* **1982**, *232*, 47. (c) Schneider, J.; Huttner, G. *Chem. Ber.* **1983**, *116*, 917.
(24) Lesch, D. A.; Rauchfuss, T. B. *Organometallics* **1982**, *1*, 499.
(25) (a) Cotton, F. A.; Wilkinson, G. *Advanced Inorganic Chemistry*, 3rd ed.; Wiley: New York, 1972; Chapter 22. (b) Purcell, K. F.; Kotz, J. C. *Inorganic Chemistry*; W. B. Saunders: Philadelphia, 1977; Chapter 18. (c) Cotton, F. A.; Kraihanzel, C. S. *J. Am. Chem. Soc.* **1962**, *84*, 4432.
(26) Richmond, M. G.; Korp, J. D.; Kochi, J. K., manuscript in preparation.

**Table IV.** Fractional Positional Parameters for the Non-Hydrogen Atoms of $Co_4(CO)_6[P(OMe)_3]_4(PPh)_2$

| atom | x | y | z | B, Å² | atom | x | y | z | B, Å² |
|---|---|---|---|---|---|---|---|---|---|
| Co1 | 0.6018 (1) | 0.4986 (1) | 0.42082 (7) | 2.43 (3) | C2 | 0.4346 (9) | 0.7177 (8) | 0.4251 (6) | 3.9 (3) |
| Co2 | 0.4208 (1) | 0.5616 (1) | 0.43224 (7) | 2.54 (3) | C3 | 0.5298 (9) | 0.5698 (7) | 0.3496 (5) | 3.3 (3) |
| Co3 | 0.1239 (1) | 0.0017 (1) | 0.06674 (7) | 2.22 (3) | C4 | 0.464 (1) | 0.3065 (9) | 0.2353 (6) | 5.1 (3) |
| Co4 | −0.0556 (1) | 0.0669 (1) | 0.08034 (7) | 2.17 (3) | C5 | 0.573 (1) | 0.1123 (9) | 0.3923 (8) | 8.6 (4) |
| P1 | 0.5773 (2) | 0.6118 (2) | 0.5194 (1) | 2.33 (7) | C6 | 0.773 (1) | 0.325 (1) | 0.2546 (7) | 6.8 (4) |
| P2 | 0.6146 (3) | 0.3470 (2) | 0.3546 (2) | 3.56 (8) | C7 | 0.009 (1) | 0.286 (1) | 0.3924 (8) | 7.6 (4) |
| P3 | 0.2354 (3) | 0.4760 (2) | 0.3804 (2) | 3.57 (8) | C8 | 0.135 (1) | 0.6232 (9) | 0.4348 (7) | 6.3 (3) |
| P4 | −0.0722 (2) | −0.1103 (2) | 0.0187 (1) | 2.17 (7) | C9 | 0.235 (1) | 0.481 (1) | 0.2334 (7) | 10.0 (5) |
| P5 | 0.1429 (2) | −0.1475 (2) | 0.1240 (2) | 3.35 (7) | C10 | 0.6899 (8) | 0.7750 (7) | 0.5360 (5) | 2.3 (2) |
| P6 | −0.2269 (2) | −0.0070 (2) | 0.1436 (2) | 3.02 (7) | C11 | 0.7268 (9) | 0.8525 (8) | 0.4770 (5) | 3.5 (3) |
| O1 | 0.8652 (6) | 0.6710 (6) | 0.4021 (4) | 5.7 (2) | C12 | 0.811 (1) | 0.9756 (8) | 0.4872 (6) | 4.6 (3) |
| O2 | 0.4372 (7) | 0.8139 (6) | 0.4178 (5) | 7.6 (3) | C13 | 0.863 (1) | 1.0224 (8) | 0.5577 (6) | 4.6 (3) |
| O3 | 0.5489 (6) | 0.6106 (6) | 0.2899 (4) | 5.0 (2) | C14 | 0.8276 (9) | 0.9463 (8) | 0.6175 (5) | 3.9 (3) |
| O4 | 0.5063 (6) | 0.2554 (5) | 0.2959 (4) | 4.5 (2) | C15 | 0.7421 (8) | 0.8241 (8) | 0.6064 (5) | 3.2 (3) |
| O5 | 0.6322 (7) | 0.2436 (5) | 0.4009 (4) | 6.5 (2) | C16 | 0.2863 (8) | 0.0993 (7) | 0.0617 (5) | 2.8 (3) |
| O6 | 0.7370 (6) | 0.4018 (6) | 0.3051 (4) | 5.4 (2) | C17 | −0.0360 (8) | 0.2240 (8) | 0.0943 (5) | 2.7 (3) |
| O7 | 0.1344 (6) | 0.3599 (6) | 0.4206 (4) | 5.2 (2) | C18 | 0.0769 (8) | 0.0807 (7) | 0.1510 (5) | 2.5 (3) |
| O8 | 0.1637 (6) | 0.5652 (5) | 0.3689 (4) | 5.2 (2) | C19 | 0.056 (1) | −0.283 (1) | 0.2454 (6) | 7.3 (4) |
| O9 | 0.2208 (7) | 0.4192 (6) | 0.2968 (4) | 5.9 (2) | C20 | 0.146 (1) | −0.365 (1) | 0.0713 (7) | 8.4 (4) |
| O16 | 0.3934 (5) | 0.1588 (6) | 0.0578 (4) | 4.3 (2) | C21 | 0.341 (1) | −0.039 (1) | 0.2115 (7) | 5.8 (4) |
| O17 | −0.0307 (6) | 0.3219 (5) | 0.1066 (4) | 5.1 (2) | C22 | −0.452 (1) | −0.2044 (9) | 0.1473 (7) | 5.5 (3) |
| O18 | 0.1149 (6) | 0.1228 (5) | 0.2109 (3) | 4.0 (2) | C23 | −0.170 (1) | −0.084 (1) | 0.2687 (6) | 5.8 (4) |
| O19 | 0.0614 (6) | −0.1878 (5) | 0.1971 (3) | 4.4 (2) | C24 | −0.3493 (9) | 0.1065 (9) | 0.0773 (7) | 5.4 (3) |
| O20 | 0.1067 (6) | −0.2719 (5) | 0.0721 (4) | 5.3 (2) | C25 | −0.1811 (7) | −0.2723 (7) | 0.0334 (5) | 2.1 (2) |
| O21 | 0.2796 (6) | −0.1300 (6) | 0.1520 (4) | 4.9 (2) | C26 | −0.2017 (8) | −0.3200 (8) | 0.1040 (5) | 3.5 (3) |
| O22 | −0.3269 (5) | −0.1417 (5) | 0.1160 (4) | 3.8 (2) | C27 | −0.287 (1) | −0.4424 (9) | 0.1136 (6) | 5.2 (3) |
| O23 | −0.2219 (6) | −0.0086 (6) | 0.2336 (4) | 4.9 (2) | C28 | −0.352 (1) | −0.5167 (8) | 0.0521 (7) | 5.5 (3) |
| O24 | −0.3067 (5) | 0.0759 (5) | 0.1461 (4) | 4.1 (2) | C29 | −0.3341 (9) | −0.4714 (8) | −0.0171 (6) | 4.7 (3) |
| C1 | 0.7613 (9) | 0.6023 (8) | 0.4106 (5) | 3.4 (3) | C30 | −0.2481 (8) | −0.3488 (8) | −0.0277 (5) | 3.1 (3) |

**Table V.** Selected Distances (Å) and Bond Angles (deg) in $Co_4(CO)_8[P(OMe)_3]_2(PPh)_2$ (III)[a]

| | | | |
|---|---|---|---|
| Co1–Co2 | 2.524 (1) | Co2–C3 | 1.775 (4) |
| Co1–Co2′ | 2.713 (1) | Co2–C4 | 2.012 (4) |
| Co1–P1 | 2.250 (1) | C1–O1 | 1.151 (4) |
| Co2–P1 | 2.254 (1) | C2–O2 | 1.135 (4) |
| Co1–P2 | 2.169 (1) | C3–O3 | 1.141 (4) |
| Co1–C1 | 1.770 (4) | C4–O4 | 1.166 (4) |
| Co1–C4 | 1.882 (4) | P1–C8 | 1.821 (3) |
| Co2–C2 | 1.788 (4) | P1···P1′ | 2.534 (2) |
| Co2–Co1–Co2′ | 90.25 (2) | P1–Co2–P1′ | 68.60 (4) |
| Co1–Co2–Co1′ | 89.75 (2) | Co1–C4–Co2 | 80.7 (2) |
| Co1–P1–Co2 | 68.39 (3) | Co1–C1–O1 | 176.8 (4) |
| Co1′–P1–Co2′ | 74.09 (3) | Co2–C2–O2 | 175.2 (3) |
| Co1–P1–Co2′ | 68.39 (3) | Co2–C3–O3 | 177.8 (3) |
| Co2–P1–Co1′ | 74.09 (3) | P1′–Co1–P2 | 96.22 (4) |
| Co1–P1–Co1′ | 111.17 (4) | | |
| Co2–P1–Co2′ | 111.40 (4) | | |
| P1–Co1–P1′ | 68.83 (4) | | |

[a] Numbers in parentheses are estimated standard deviations in the least significant digit.

**Table VI.** Selected Distances (Å) and Bond Angles (deg) in $Co_4(CO)_6[P(OMe)_3]_4(PPh)_2$ (V)[a]

| | | | |
|---|---|---|---|
| Co1–Co2 | 2.518 (1) | Co1–C1 | 1.760 (9) |
| Co2–Co1′ | 2.727 (1) | Co2–C2 | 1.784 (9) |
| Co3–Co4 | 2.521 (1) | Co3–C16 | 1.760 (9) |
| Co2–Co4 | 2.726 (1) | Co4–C17 | 1.773 (9) |
| Co1–P1 | 2.259 (2) | Co1–C3 | 1.913 (8) |
| Co2–P1 | 2.249 (2) | Co2–C3 | 1.934 (8) |
| Co3–P4 | 2.246 (2) | Co3–C18 | 1.940 (8) |
| Co4–P4 | 2.255 (2) | Co4–C18 | 1.932 (8) |
| Co1–P2 | 2.161 (2) | P1–C10 | 1.827 (6) |
| Co2–P3 | 2.145 (2) | P4–C25 | 1.825 (7) |
| Co3–P5 | 2.151 (2) | P1···P1′ | 2.554 (3) |
| Co4–P6 | 2.162 (2) | P4···P4′ | 2.553 (3) |
| Co2–Co1–Co2′ | 89.91 (4) | P1–Co2–P1′ | 69.11 (8) |
| Co1–Co2–Co1′ | 90.09 (4) | P4–Co3–P4′ | 69.09 (7) |
| Co4–Co3–Co4′ | 90.12 (4) | P4–Co4–P4′ | 68.97 (7) |
| Co3–Co4–Co3′ | 89.88 (4) | Co1–C3–Co2 | 81.8 (3) |
| Co1–P1–Co2 | 67.91 (6) | Co3–C18–Co4 | 81.3 (3) |
| Co1–P1–Co2′ | 74.36 (6) | Co1–C1–O1 | 178.2 (7) |
| Co3–P4–Co4 | 68.12 (6) | Co2–C2–O2 | 175.9 (7) |
| Co3–P4–Co4′ | 74.55 (6) | Co3–C16–O16 | 177.2 (7) |
| Co1–P1–Co1′ | 110.97 (8) | Co4–C17–O17 | 175.0 (6) |
| Co2–P1–Co2′ | 110.89 (8) | P1′–Co1–P2 | 98.73 (8) |
| Co3–P4–Co3′ | 110.91 (7) | P1′–Co2–P3 | 97.63 (8) |
| Co4–P4–Co4′ | 111.03 (7) | P4′–Co3–P5 | 97.10 (8) |
| P1–Co1–P1′ | 69.03 (8) | P4′–Co4–P6 | 99.63 (7) |

[a] Distances and lengths for the two half-molecules in the unit cell. Numbers in parentheses are estimated standard deviations in the least significant digit.

centration is presented in Figure 4. The intercepts and the slopes afford the ligand-independent and the ligand-dependent rate constants $k_1$ and $k_2$, respectively (Table VIII).

The effects of radical traps and carbon monoxide on the pseudo-first-order rate constant for ligand substitution were also investigated. For example, the kinetics study in the presence of tri-*n*-butyltin hydride is included in Table VI (entry 6). This additive has been shown to be an efficient inhibitor of free-radical-chain processes involving other metal carbonyls.[27] Furthermore, tri-*n*-butyltin hydride effectively terminates the ETC catalysis of ligand substitution in $Co_4(CO)_{10}(PPh)_2$.[15] Thus the inability of tri-*n*-butyltin hydride to affect the rate of ligand substitution constitutes proof that eq 2 occurs via a purely thermal process. The effect of added carbon monoxide on the rate of ligand substitution of $Co_4(CO)_{10}(PPh)_2$ is also included in Table VII. Entry 14 shows that the observed pseudo-first-order rate constant remains essentially unaffected in the presence of 1 atm of CO.

**B. Bis-substitution** of the tetracobalt cluster was examined with $Co_4(CO)_9[P(OMe)_3](PPh)_2$ (II) and a measured excess of trimethyl phosphite, i.e.

$$\underset{\text{II}}{Co_4(CO)_9[P(OMe)_3](PPh)_2} + P(OMe)_3 \rightarrow \underset{\text{III}}{Co_4(CO)_8[P(OMe)_3]_2(PPh)_2} + CO \quad (3)$$

The reaction followed first-order kinetics for at least 3 half-lives over the temperature range between 30 and 54 °C. The pseudo-first-order rate constants ($k_{obsd}$) in Table IX increase linearly with phosphite concentration, as shown in Figure 5. The lig-

(27) (a) Narayanan, B. A.; Amatore, C.; Casey, C. P.; Kochi, J. K. *J. Am. Chem. Soc.* **1983**, *105*, 6351. (b) Narayanan, B. A.; Amatore, C.; Kochi, J. K. *Organometallics* **1984**, *3*, 802.

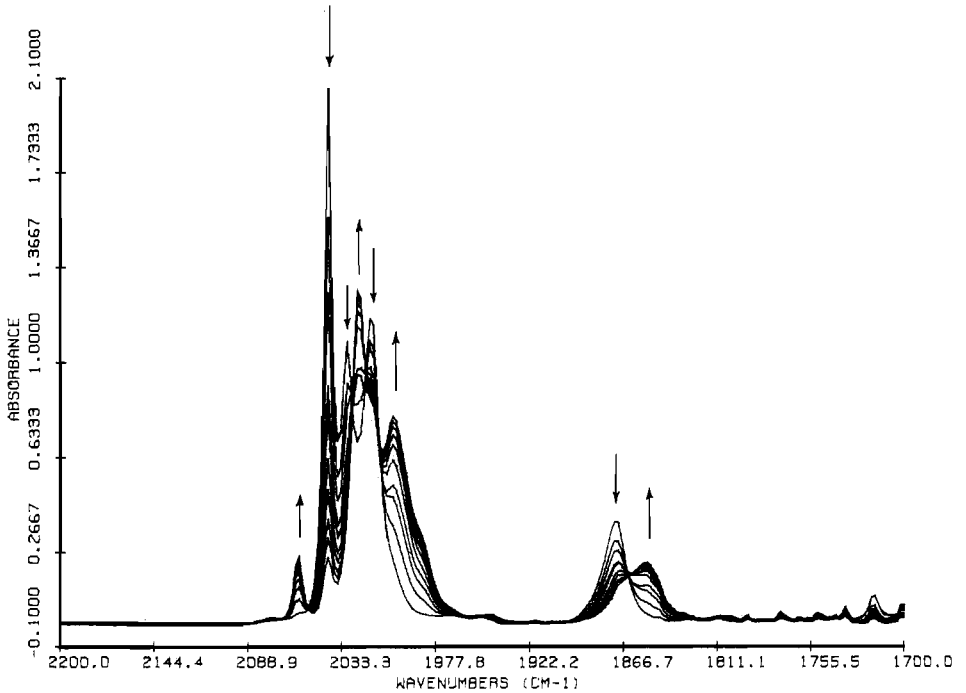


**Figure 3.** Typical changes in the infrared spectrum accompanying the ligand substitution of $Co_4(CO)_{10}(\mu_4\text{-}PPh)_2$ (I) with trimethyl phosphite to afford $Co_4(CO)_9[P(OMe)_3](\mu_4\text{-}PPh)_2$ (II).

**Table VII.** Experimental Rate Constants for the (Mono) Ligand Substitution of $Co_4(CO)_{10}(PPh)_2$ (I) with Trimethyl Phosphite[a]

| entry no. | temp, °C | $10^2[P(OMe)_3]$, M | $10^5k_{obsd}$,[b] $s^{-1}$ | entry no. | temp, °C | $10^2[P(OMe)_3]$, M | $10^5k_{obsd}$,[b] $s^{-1}$ |
|---|---|---|---|---|---|---|---|
| 1 | 15.3 | 40.0 | 14.7 ± 4.8 | 11 | 30.2 | 80.3 | 123.0 ± 31.6 |
| 2 | 15.3 | 49.7 | 18.8 ± 1.9 | 12 | 35.7 | 11.0 | 57.6 ± 9.2 |
| 3 | 15.3 | 80.0 | 25.7 ± 5.6 | 13 | 35.7 | 16.9 | 65.6 ± 13.0 |
| 4 | 23.5 | 25.0 | 20.8 ± 1.3 | 14 | 35.7 | 16.9 | 64.8 ± 4.4[d] |
| 5 | 23.5 | 55.7 | 39.5 ± 7.6 | 15 | 35.7 | 53.8 | 163.2 ± 47.3 |
| 6 | 23.5 | 55.7 | 54.5 ± 8.2[c] | 16 | 35.7 | 80.7 | 219.7 ± 53.8 |
| 7 | 23.5 | 88.0 | 59.0 ± 9.3 | 17 | 42.2 | 10.0 | 78.4 ± 6.5 |
| 8 | 30.2 | 9.7 | 25.7 ± 2.4 | 18 | 42.2 | 17.5 | 121.0 ± 5.3 |
| 9 | 30.2 | 16.8 | 33.7 ± 4.9 | 19 | 42.2 | 25.0 | 141.0 ± 21.2 |
| 10 | 30.2 | 27.0 | 50.4 ± 7.9 | 20 | 42.2 | 33.2 | 183.0 ± 7.1 |

[a] From $1.0 \times 10^{-2}$ M $Co_4(CO)_{10}(PPh)_2$ in toluene by following the disappearance of the IR band at 2040.8 $cm^{-1}$. [b] Error limits at 95% confidence level. [c] In the presence of 0.04 M tri-*n*-butyltin hydride. [d] In the presence of 1 atm of CO.

**Table VIII.** Ligand-Independent and Ligand-Dependent Rate Constants for the Ligand Substitution of $Co_4(CO)_{10}(PPh)_2$ (I) with Trimethyl Phosphite[a]

| temp, °C | $10^5k_1$, $s^{-1}$ | $10^4k_2$, $M^{-1}$ $s^{-1}$ |
|---|---|---|
| 15.3 | 4.8 ± 2.0 | 2.6 ± 0.4 |
| 23.5 | 5.7 ± 0.07 | 6.1 ± 0.01 |
| 30.2 | 11.8 ± 1.5 | 13.9 ± 0.3 |
| 35.7 | 29.4 ± 6.9 | 23.9 ± 1.4 |
| 42.2 | 38.0 ± 8.2 | 43.3 ± 3.0 |

[a] From Figure 4. Error limits are at the 95% confidence level.

and-independent and the ligand-dependent rate constants $k_1$ and $k_2$, respectively, are included in Table X. When the ligand substitution is carried out under these conditions, the changes in the infrared spectra show a clean conversion to only the bis(phosphite) derivative III similar to that shown in Figure 3 for the mono(phosphite) derivative II. The effects of additives such as tri-*n*-butyltin hydride and carbon monoxide (Table IX, entries 5 and 6) were similar to those observed in the first substitution step. Thus the second substitution step also arises from a thermal process without any radical-chain character.

**C. Tris-substitution** of the tetracobalt cluster was examined with $Co_4(CO)_8[P(OMe)_3]_2(PPh)_2$ (III) and a measured amount of trimethyl phosphite, i.e.

$$\underset{\text{III}}{Co_4(CO)_8[P(OMe)_3]_2(PPh)_2} + P(OMe)_3 \rightarrow \underset{\text{IV}}{Co_4(CO)_7[P(OMe)_3]_3(PPh)_2} + CO \quad (4)$$

**Table IX.** Observed Rate Constants for the (Bis) Ligand Substitution of $Co_4(CO)_9[P(OMe)_3](PPh)_2$ (II) with Trimethyl Phosphite[a]

| entry no. | temp, °C | 10[P(OMe)], M | $10^5k_{obsd}$,[b] $s^{-1}$ | entry no. | temp, °C | 10[P(OMe)], M | $10^5k_{obsd}$,[b] $s^{-1}$ |
|---|---|---|---|---|---|---|---|
| 1 | 30.2 | 11.6 | 13.0 ± 0.4 | 8 | 38.3 | 22.9 | 49.6 ± 0.7 |
| 2 | 30.2 | 26.9 | 26.1 ± 0.3 | 9 | 46.3 | 7.0 | 40.1 ± 1.1 |
| 3 | 30.2 | 43.0 | 37.2 ± 0.5 | 10 | 46.3 | 9.4 | 53.2 ± 2.2 |
| 4 | 38.3 | 7.0 | 20.9 ± 0.2 | 11 | 46.3 | 11.0 | 56.7 ± 1.4 |
| 5 | 38.3 | 7.0 | 19.5 ± 0.3[c] | 12 | 53.5 | 7.0 | 79.8 ± 1.5 |
| 6 | 38.3 | 7.0 | 20.0 ± 0.1[d] | 13 | 53.5 | 10.2 | 103.3 ± 1.6 |
| 7 | 38.3 | 14.8 | 32.8 ± 0.5 | 14 | 53.5 | 13.4 | 125.4 ± 4.2 |

[a] From $5 \times 10^{-2}$ M $Co_4(CO)_9[P(OMe)_3](PPh)_2$ (II) in toluene by following the disappearance of the IR band at 2058.4 $cm^{-1}$. [b] Error limits at 95% confidence level. [c] In the presence of 0.04 M tri-*n*-butyltin hydride. [d] In the presence of 1 atm of CO.

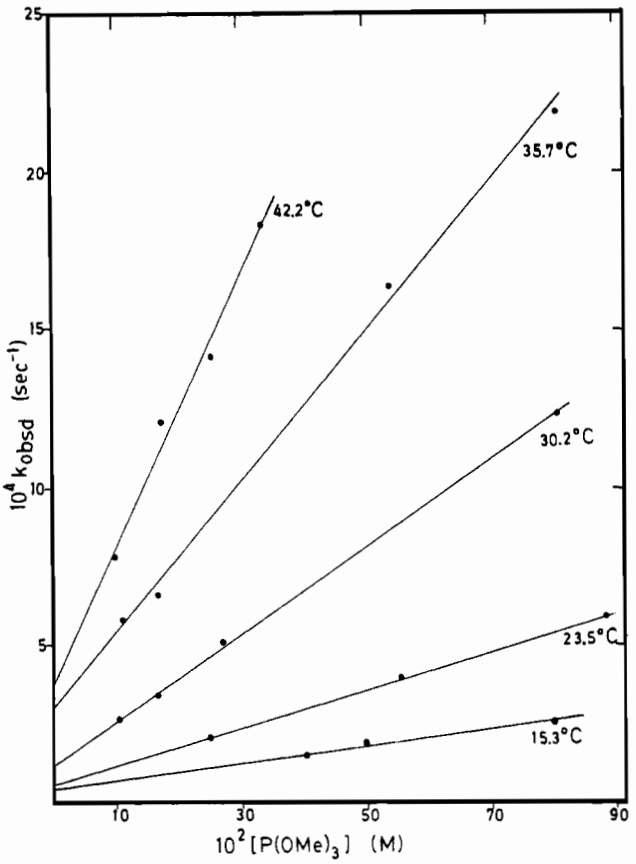


**Figure 4.** Dependence of the observed first-order rate constant $k_{obsd}$ for ligand substitution of $Co_4(CO)_{10}(\mu_4\text{-}PPh)_2$ (I) on the concentration of trimethyl phosphite at various temperatures, as indicated.

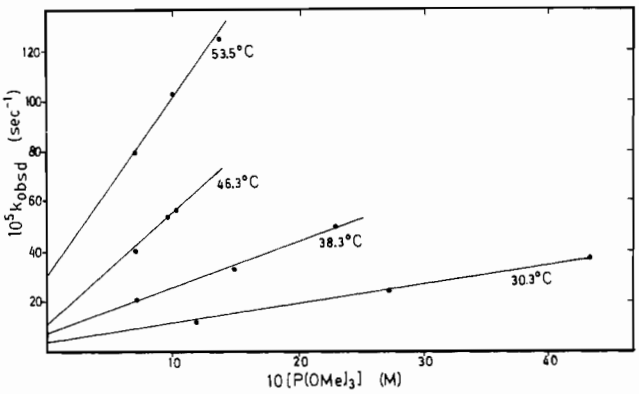


**Figure 5.** Dependence of the observed first-order rate constant $k_{obsd}$ for ligand substitution of $Co_4(CO)_9[P(OMe)_3](\mu_4\text{-}PPh)_2$ (II) on the concentration of trimethyl phosphite at various temperatures, as indicated.

**Table X.** Ligand-Independent and Ligand-Dependent Rate Constants for the Ligand Substitution of $Co_4(CO)_9[P(OMe)_3](PPh)_2$ (II) Trimethyl Phosphite[a]

| temp, °C | $10^5 k_1$, s$^{-1}$ | $10^5 k_2$, M$^{-1}$ s$^{-1}$ |
|---|---|---|
| 30.2 | 4.4 ± 4.1 | 7.8 ± 1.4 |
| 38.3 | 7.5 ± 7.9 | 18.1 ± 4.5 |
| 46.3 | 11.2 ± 7.6 | 42.5 ± 4.3 |
| 53.5 | 30.7 ± 4.0 | 70.7 ± 1.4 |

[a] From Figure 5. Error limits are at the 95% confidence level.

The reaction followed pseudo-first-order kinetics for at least 3 half-lives over the temperature range between 51 and 76 °C. Ligand substitution under these conditions however is not selective, since an inspection of the infrared spectra shows the evolution initially of the tris(phosphite) derivative IV and then the tetrakis(phosphite) derivtive V as the reaction progresses. Thus the rates of the third and fourth ligand substitutions are comparable.

**Table XI.** Rate Constants for the (Tris) Ligand Substitution of $Co_4(CO)_8[P(OMe)_3]_2(PPh)_2$ (III) with Trimethyl Phosphite[a]

| entry no. | temp, °C | $10[P(OMe)_3]$, M | $10^4 k_{obsd}$,[b] s$^{-1}$ |
|---|---|---|---|
| 1 | 51.1 | 1.01 | 0.70 ± 0.05 |
| 2 | 62.4 | 7.13 | 3.3 ± 0.7 |
| 3 | 62.4 | 18.3 | 3.6 ± 0.2 |
| 4 | 62.4 | 37.4 | 3.9 ± 0.6 |
| 5 | 69.1 | 10.1 | 8.2 ± 0.3 |
| 6 | 75.7 | 10.4 | 17.9 ± 0.5 |

[a] From $4.7 \times 10^{-2}$ M $Co_4(CO)_8[P(OMe)_3]_2(PPh)_2$ in toluene by following the IR band at 2038.9 cm$^{-1}$. [b] Error limits are at the 95% confidence level.

**Table XII.** Rate Constants for (Tetrakis) Ligand Substitution of $Co_4(CO)_7[P(OMe)_3]_3(PPh)_2$ with Trimethyl Phosphite[a]

| entry no. | temp, °C | $10^2[P(OMe)_3]$, M | $10^4 k_{obsd}$,[b] s$^{-1}$ |
|---|---|---|---|
| 1 | 55.5 | 24.2 | 0.7 ± 0.02 |
| 2 | 62.5 | 17.1 | 1.8 ± 0.06 |
| 3 | 62.5 | 60.5 | 1.7 ± 0.2 |
| 4 | 72.5 | 27.2 | 8.0 ± 1.1 |
| 5 | 78.0 | 30.2 | 13.4 ± 1.0 |

[a] From $1.5 \times 10^{-2}$ M $Co_4(CO)_7[P(OMe)_3]_3(PPh)_2$ in toluene by following the IR band at 2015.4 cm$^{-1}$. [b] Error limits are at the 95% confidence level.

The observed first-order rate constant is also insensitive to the concentrations of trimethyl phosphite, as shown in Table XI, entries 2–4. Such a ligand-independent behavior of the third step is consistent with a dissociative loss of CO in the activation process.

**D. Tetrakis-substitution** of the tetracarbonyl cluster was examined with $Co_4(CO)_7[P(OMe)_3]_3(PPh)_2$ (IV) and a measured excess of trimethyl phosphite, i.e.

$$\underset{\text{IV}}{Co_4(CO)_7[P(OMe)_3]_3(PPh)_2} + P(OMe)_3 \rightarrow \underset{\text{V}}{Co_4(CO)_6[P(OMe)_3]_4(PPh)_2} + CO \quad (5)$$

The reaction followed first-order kinetics for at least 3 half-lives over the temperature range 55–78 °C. The pseudo-first-order rate constants in Table XII represent the clean conversion to only the tetrakis(phosphite) derivative V ($n = 4$). The insensitivity of the rate constant to variations in the phosphite concentration is the same as that observed for tris-substitution. No further substitution was observed even after prolonged periods.

**IV. Temperature-Dependent Behavior of Tetracobalt Clusters.** When a solution of the parent tetracobalt cluster I in benzene is exposed to an atmosphere of $^{13}C$-labeled carbon monoxide at 50 °C, there is a small amount of isotopic incorporation (~5%) only after prolonged periods. Similar results were obtained with the phosphite derivatives II, III, and IV with $n = 1$–3. Thus the intermolecular exchanges of CO ligands in these tetracobalt clusters are rather slow. By comparison, the intramolecular exchange of carbon monoxide between the terminal and bridging positions occurs on the NMR time scale. For example, the limiting $^{13}C$ NMR spectrum of the parent cluster I at 173 K in Figure 6 shows two resonances at $\delta$ 238.0 and 203.9 with relative intensities of 1:4, which are readily assigned to the pair of bridging CO's and the eight equivalent terminal CO's, respectively, for the parent cluster possessing idealized $D_{2h}$ symmetry. As the temperature is raised, both resonances broaden more or less simultaneously, and they finally merge to a single broad resonance at 273 K. The observed chemical shift at $\delta$ 208 of the broadened signal is in good agreement with the weighted average chemical shifts of the terminal and bridging carbonyls. Such a temperature-dependent behavior of the $^{13}C$ NMR spectra is characteristic of a rapid bridge–terminal carbonyl interchange via a mutual exchange mechanism[28] of the type involving a one-for-one, two-

(28) For some reviews on fluxional processes in metal cluster compounds, see: (a) Band, E.; Muetterties, E. L. *Chem. Rev.* **1978**, *78*, 639. (b) Aime, S.; Milone, L. *Prog. Nucl. Magn. Reson. Spectrosc.* **1977**, *11*, 183. (c) Johnson, B. F. G.; Benfield, R. E. In *Transition Metal Clusters*; Johnson, B. F. G., Ed.; Wiley: New York, 1980; Chapter 7.

**Table XIII.** Temperature Dependence of the $^{13}C$ NMR Spectra of Tetracobalt Clusters[a]

| tetracobalt cluster | CO chem shift, ppm | | $T_c$,[b] K | $\Delta G^{\ddagger}$,[c] kcal mol$^{-1}$ |
|---|---|---|---|---|
| | terminal | bridge | | |
| $Co_4(CO)_{10}(PPh)_2$ | 203.9 | 238.6 | 273 | 11.5 |
| $Co_4(CO)_9[P(OMe)_3](PPh)_2$ | 206.0, 203.9 | 241.5, 240.8 | 298 | 12.5 |
| $Co_4(CO)_8[P(OMe)_3]_2(PPh)_2$ | 205.5 | 244.0 (248.3)[d] | 313 | 13.2 |
| $Co_4(CO)_7[P(OMe)_3]_3(PPh)_2$ | 209.8, 208.2, 206.9 | 251.9, 249.7 (253.5, 249.2)[d] | 301 | 12.8 |
| $Co_4(CO)_6[P(OMe)_3]_4(PPh)_2$ | 209.7 | 255.7 | 328 | 13.6 |

[a] $^{13}C$ spectra measured in 4:1 v/v mixture of 2-methyltetrahydrofuran/benzene-$d_6$ in the presence of 0.03 M $Cr(acac)_3$ at temperatures between 193 and 203 K. [b] Coalescence temperature. [c] See Experimental Section. [d] Minor component in parentheses.

**Chart I**

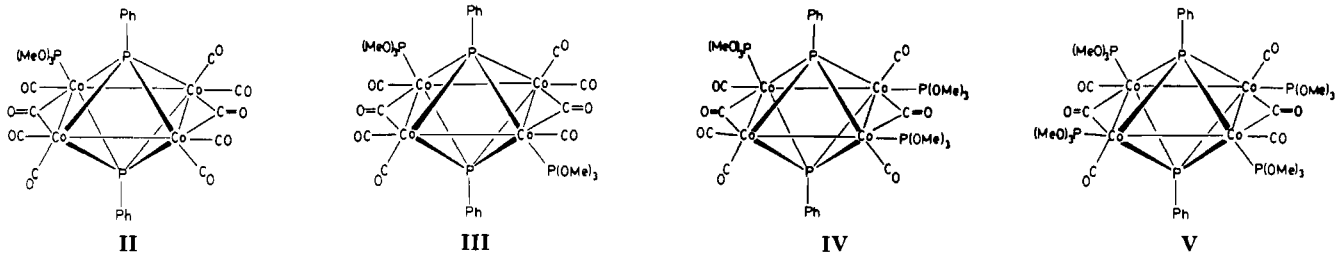


center process advocated by Lewis and co-workers for $Cp_2Rh_2(CO)_3$ and $Cp_2Rh_2(CO)_2[P(OPh)_3]$.[29,30] The variable-temperature spectral data are listed in Table XIII, together with the activation free energy evaluated for such intramolecular exchanges.[31] (For the details, see Experimental Section.)

The tetracobalt derivatives II–V (with $n$ = 1–4) all show the expected downfield shifts of both the terminal and bridging carbonyl resonances in measure with the number of phosphite ligands on the cluster. For example, the monosubstituted derivative II has resolved resonances at $\delta$ 241.5 and 240.8 for the two bridging carbonyls, the lower field signal being assigned to that adjacent to the $P(OMe)_3$ substituent. The $^{13}C$ NMR spectrum of the bis(phosphite) III ($n$ = 2) in solution at 173 K shows two resonances at $\delta$ 244.0 and 248.3 with rather disperse intensity ratios (see Figure 6). Since the predominant resonance is likely to be associated with the 1,3-trans structure shown in Figure 2a, we tentatively assign the minor resonance to the 1,3-cis isomer resulting from stereomutation in solution.[32] The tris(phosphite) IV ($n$ = 3) displays an interesting low-temperature $^{13}C$ NMR spectrum. Thus at 193 K, the pair of bridging carbonyl resonances appears in two sets with a 7:3 intensity ratio. These probably represent the two isomers observed in the unit cell of the crystal, resulting from atropisomerism about the $P(\mu_4)$–phenyl bond.[34,35] The tetrakis(phosphite) V ($n$ = 4) shows only two singlets at $\delta$ 255.7 and 209.7 for the bridging and terminal carbonyls, respectively, in the $^{13}C$ NMR spectrum, as expected for a cluster possessing idealized $C_{2h}$ symmetry (see Figure 2b). When all the data are taken together, there is a consistent trend in the $^{13}C$ NMR spectrum for the terminal carbonyl resonances to be successively shifted to lower field with increasing phosphite substitution. However, the magnitude of the overall span in chemical shift difference is rather small. In this regard, the bridging carbonyl ligands are more sensitive indicators for the extent of substitution and the location of phosphite ligands in the cluster. This correlation is to be noted in Table XIII for the parent tetracobalt cluster I and its four phosphite derivatives II–V ($n$ = 1–4). The chemical shifts of the minor isomers are indicated in parentheses.

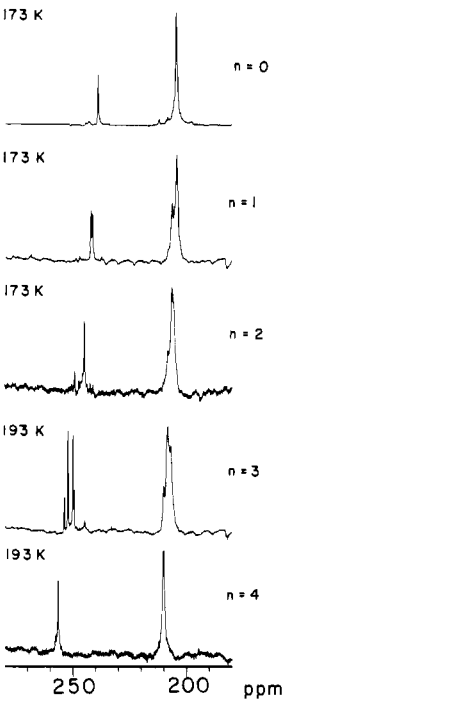


**Figure 6.** Limiting $^{13}C$ NMR spectra of the tetracobalt clusters $Co_4(CO)_{10-n}[P(OMe)_3]_n(\mu_4\text{-}PPh)_2$ with $n$ = 0–4 at the indicated temperatures.

## Discussion

The bicapped tetracobalt cluster I undergoes smooth replacement of up to four carbonyl ligands with trimethyl phosphite to afford $Co_4(CO)_{10-n}[P(OMe)_3]_n(PPh)_2$. The successful isolation of the phosphite derivatives II–V in each step of the ligand substitution according to eq 2–5 allows the individual structures with $n$ = 1–4 to be established by X-ray crystallography as represented in Chart I. We infer from the unique trends in the substitution pattern (regiochemistry) and the stereochemistry in Chart I that

(29) (a) Evans, J.; Johnson, B. F. G.; Lewis, J.; Norton, J. R. *J. Chem. Soc., Chem. Commun.* **1973**, 79. (b) Evans, J.; Johnson, B. F. G.; Lewis, J.; Matheson, T. W. *J. Chem. Soc., Chem. Commun.* **1975**, 576. (c) Evans, J.; Johnson, B. F. G.; Lewis, J.; Matheson, T. W.; Norton, J. R. *J. Chem. Soc., Dalton Trans.* **1978**, 626.

(30) Cf. also the process described in ref 28a.

(31) (a) Shanan-Atidi, H.; Bar-Eli, K. H. *J. Phys. Chem.* **1970**, *74*, 961. (b) Sandstrom, J. *Dynamic NMR Spectroscopy*; Academic: New York, 1982.

(32) It is also possible that the minor component is an atropisomer (vide infra). We disfavor a 1,2-substituted isomer.[33] See also ref 44 (vide infra).

(33) The variable-temperature $^{13}C$ NMR and IR spectra of 1,2-substituted derivatives are different, arguing against a 1,2-substituted isomer of $Co_4(CO)_8[P(OMe)_3]_2(PPh)_2$. Richmond, M. G., unpublished results.

(34) For a discussion on atropisomerism in organic compounds, see: (a) Mislow, K. *Introduction to Stereochemistry*; W. A. Benjamin: New York, 1966. (b) Eliel, E. L.; Allinger, N. L.; Angyal, S. T.; Morrison, G. A. *Conformational Analysis*; Interscience: New York, 1967. (c) Morrison, J. D.; Mosher, H. S. *Asymmetric Organic Reactions*; Prentice-Hall: New York, 1971.

(35) A full report of the single-crystal X-ray diffraction of $Co_4(CO)_7[P(OMe)_3]_3(PPh)_2$ will be presented later.

**Table XIV.** Kinetics of Ligand Substitution

| substitution | ligand independent[a] | | | ligand dependent | | |
|---|---|---|---|---|---|---|
| | $k_1$[b] | $\Delta H^\ddagger$ | $\Delta S^\ddagger$ | $k_2$[c] | $\Delta H^\ddagger$ | $\Delta S^\ddagger$ |
| mono | 6.6 (0.83) | 15 ± 3 | −25 ± 10 | 9.3 | 19.1 ± 4.6 | −8.7 ± 1.5 |
| bis | 1.8 (0.90) | 16 ± 4 | −26 ± 10 | 0.55 | 19.2 ± 1.3 | −13.9 ± 4.9 |
| tris | 0.61 (0.15) | 29.4 ± 0.9 | 14.3 ± 2.7 | <0.001[d] | | |
| tetrakis | 0.28 (0.14) | 30.6 ± 1.8 | 15.4 ± 5.4 | <0.001[d] | | |

[a] Calculated from the experimental rate data extrapolated to 50 °C. $\Delta H^\ddagger$ values are in kcal mol$^{-1}$ and $\Delta S^\ddagger$ in eu. [b] $10^4$ s$^{-1}$. Numbers in parentheses are normalized to the number of available terminal CO's. [c] $10^3$ M$^{-1}$ s$^{-1}$. [d] Extrapolated estimate of upper limit.

**Scheme I**

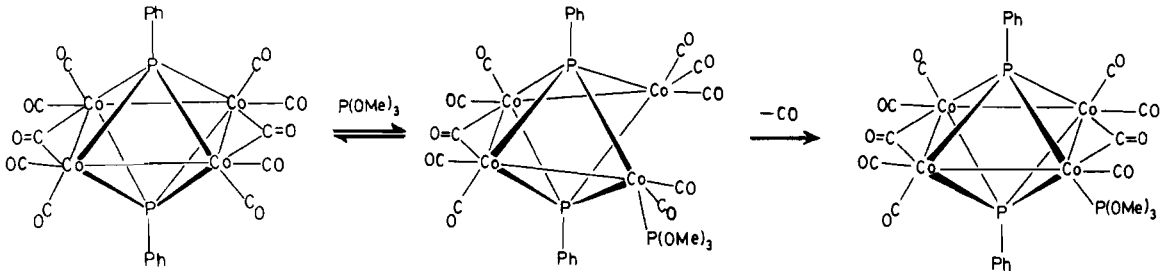


thermodynamic control plays an important role in the formation of each substitution product. For example, the bis-substitution product III ($n$ = 2) existing exclusively as the 1,3-syn/anti isomer (Figure 2a) is in accord with the second phosphite entering a trans position that is most remote from the site of the first phosphite ligand. Next, the 1,2,3-substitution pattern in the tris derivative IV with syn/anti/syn stereochemistry again places each phosphite on separate cobalt centers in an alternating arrangement for maximal interligand separation. The achievement of this stereochemistry requires an accompanying stereomutation from trans to cis of the 1,3-pair of phosphite ligands. Finally, the 1,2,3,4-substitution pattern in the tetrakis derivative V with syn/syn/anti/anti stereochemistry minimizes the combined steric interactions between the phosphite ligands and the $\mu_4$-phenylphosphinidene caps at the slight expense of a pair of cis interactions of phosphite ligands (vide infra). The X-ray crystal structures of the bis- and tetrakis(phosphite) derivatives III and V reveal no major alteration of the $Co_4P_2$ core upon substitution of CO with $P(OMe)_3$. By contrast, the only other reported phosphine derivative,[36] that obtained from triphenylphosphine as the bis-substitution product $Co_4(CO)_8(PPh_3)_2(PPh)_2$, shows substantial elongations of the Co–Co bond (non-carbonyl bridged) and the Co–P($\mu_4$) distances as a result of steric interactions between the pair of bulky cis ligands and the cluster framework. These steric interactions are minor in the corresponding substitution product from the smaller trimethyl phosphite (and even in the tetrakis(phosphite) derivative), where the ligand–cluster interactions are minimized by the favorable geometric dispositions. The importance of the phosphite disposition on cluster alteration (i.e. stability) is however observed in the tris(phosphite) derivative, in which there is significant lengthening of the Co–Co bond (non-carbonyl bridged) and a puckering of the tetracobalt plane away from planarity. We suggest that the cis orientation of the 1,3-$P(OMe)_3$ ligands in $Co_4(CO)_7[P(OMe)_3]_3(PPh)_2$ (IV) is responsible for such a distortion, similar to that present in the bis(triphenylphosphine) derivative $Co_4(CO)_8(PPh_3)_2(PPh)_2$.

Such structural analyses of the individual clusters together with the fluxional behavior of the carbonyl ligands can be integrated with the diverse kinetics behavior associated with each step leading to the multiple ligand substitution. For example, the competing first-order and second-order kinetic processes for ligand substitution are expressed by the phosphite-independent and the phosphite-dependent rate constants obtained from the intercepts and slopes, respectively, in Figures 4 and 5, i.e.

$$\text{rate} = (k_1 + k_2[P(OMe)_3])[\text{cluster}] \quad (6)$$

for mono- and bis-substitution according to eq 2 and 3.[37-43] Moreover, the insensitivity of the rate of tris- and tetrakis-substitution to the concentration of $P(OMe)_3$ indicates that $k_1 >> k_2[P(OMe)_3]$ in these later steps, as presented in eq 4 and 5. The contribution of first-order and the second-order processes at various stages of substitution is emphasized by the trends in the rate constants summarized in Table XIV.

The ligand-dependent process ($k_2$) constitutes the dominant route for mono- and bis-substitution of the tetracobalt cluster leading to II and III, respectively. For example, in the substitution of $Co_4(CO)_{10}(PPh)_2$ (I) and $Co_4(CO)_9[P(OMe)_3](PPh)_2$ (II) ($n$ = 1), the ligand-independent term accounts for ~8% and 30%, respectively, of the observed rate at 1.0 M $P(OMe)_3$.[44] Thus the predominant mode of ligand substitution in the first two steps as indicated by the observed rate law and the activation parameters (i.e., the negative entropy of activation in Table XIV) involves $P(OMe)_3$ attack on the intact cluster. We suggest that such a ligand substitution occurs by the initial addition of $P(OMe)_3$ to the cluster with concomitant scission of the carbonyl-bridged Co–Co bond. (The preferential formation of the open cluster in

(36) Ryan, R. C.; Pittman, C. U.; O'Connor, J. P.; Dahl, L. F. *J. Organomet. Chem.* **1980**, *193*, 247.

(37) For similar rate laws in inorganic and organometallic substitutions see: (a) Basolo, F.; Pearson, R. G. *Mechanisms of Inorganic Reactions*; Wiley: New York, 1967. (b) Wilkins, R. G. *The Study of Kinetics and Mechanisms of Transition Metal Complexes*; Allyn and Bacon: Boston, MA, 1974. (c) Atwood, J. D. *Inorganic and Organometallic Reaction Mechanisms*; Brooks/Cole: Monterey, CA, 1985. (d) Darensbourg, D. J. *Adv. Organomet. Chem.* **1982**, *21*, 113.

(38) For cluster substitutions, see: (a) Cetini, G.; Stanghellini, P. L.; Rossetti, R.; Gamabino, O. *Inorg. Chim. Acta* **1968**, *2*, 433. (b) Cetini, G.; Stanghellini, P. L.; Rossetti, R.; Gamabino, O. *Inorg. Chim. Acta* **1972**, *6*, 205. (c) Rossetti, R.; Gervasio, G.; Stanghellini, P. L. *J. Chem. Soc., Dalton Trans.* **1978**, 222. See also ref 39–42.

(39) (a) Candlin, J. P.; Shortland, A. C. *J. Organomet. Chem.* **1969**, *16*, 289. (b) Sonnenberger, D.; Atwood, J. D. *J. Am. Chem. Soc.* **1980**, *102*, 3484. (c) Sonnenberger, D., Atwood, J. D. *Inorg. Chem.* **1981**, *20*, 3243. (d) Sonnenberger, D.; Atwood, J. D. *J. Am. Chem. Soc.* **1982**, *104*, 2113.

(40) (a) Haines, L. I. B.; Hopgood, D.; Poe, A. J. *J. Chem. Soc. A* **1968**, 421. (b) Haines, L. I. B.; Poe, A. J. *J. Chem. Soc. A* **1969**, 2826. (c) Fawcett, J. P.; Jackson, R. A.; Poe, A. *J. Chem. Soc., Dalton Trans.* **1978**, 789.

(41) Karel, K. J.; Norton, J. R. *J. Am. Chem. Soc.* **1974**, *96*, 6812.

(42) (a) Darensbourg, D. J.; Incorvia, M. J. *J. Organomet. Chem.* **1979**, *171*, 89. (b) Darensbourg, D. J.; Incorvia, M. J. *Inorg. Chem.* **1980**, *19*, 2585.

(43) See also: (a) Angelici, R. J. *Organomet. Chem. Rev., Sect. A* **1968**, *3*, 173. (b) Corey, W. D.; Brown, T. L. *Inorg. Chem.* **1973**, *12*, 2820. (c) Cohen, M. A.; Brown, T. L. *Inorg. Chem.* **1976**, *15*, 1417. (d) Pardue, J. E.; Dobson, G. R. *Inorg. Chim. Acta* **1976**, *20*, 207. (e) Dobson, G. R. *Acc. Chem. Res.* **1976**, *9*, 300.

(44) Note that the ligand-dependent and -independent processes may lead to the different bis-substitution products noted in Chart I.[32] It is also possible that equilibration of the coordinatively unsaturated intermediate in the $k_1$ route (Scheme II) could lead to the same product as that formed in the $k_2$ route (Scheme I).

**Scheme II**

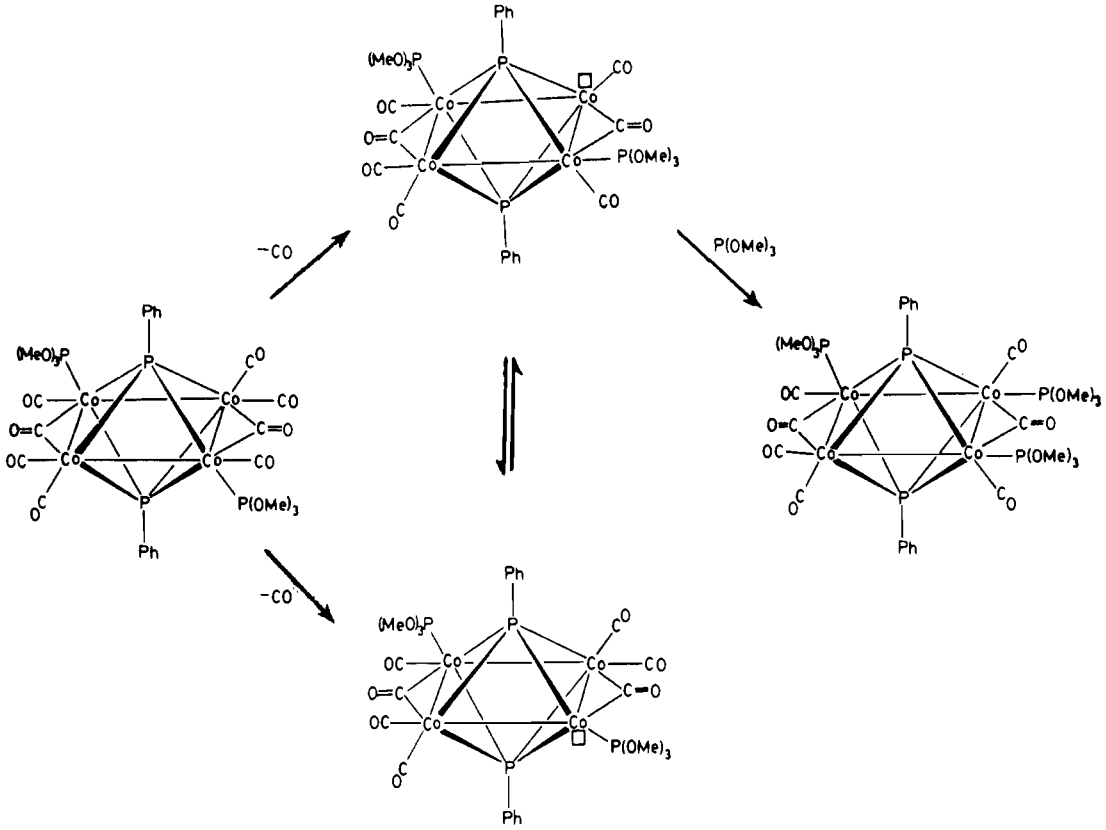

Scheme I is guided by the application of the Wade–Mingos rules.[45]) Experimental support for such a nucleophile-induced scission of the cobalt–cobalt bond derives from the tellurium-capped analogue $Co_4(CO)_{10}(\mu_4\text{-Te})_2$, which undergoes a similar tetracobalt-ring opening reversibly in the presence of added carbon monoxide.[46] The intermediate in the latter study is akin to that included in Scheme I, and it may be even longer lived owing to a larger atomic radius of the $\mu_4$-Te cap relative to the $\mu_4$-PPh cap.[47] We have recently observed an analogous ligand-induced scission of the Co–Co bond in I by the bidentate fluorophosphate ligand $(PF_2)_2NCH_3$.[48] The widened OC–Co–CO bond angle of ~105° in clusters such as I and II ($n$ = 1) will permit a facile approach of $P(OMe)_3$ required for nucleophilic scission. Such a rate-limiting associative process is consistent with the overall negative entropy of activation listed in Table XIV.[49] Accordingly, the loss of CO and ring reclosure to the substitution products II and III would occur in a subsequent, fast step. This mechanism underscores the potential of capped polynuclear clusters to act as intact entities in substitution reactions, substrate activation, and catalysis through the generation of vacant coordination sites created by metal–metal bond scission.[50]

Coordinative unsaturation in the cluster can also be generated by a dissociative loss of a CO ligand. As shown in Table XIV, the ligand-independent process ($k_1$) constitutes the dominant route for tris- and tetrakis-substitution of the tetracobalt cluster leading to IV and V, respectively. Indeed, the contribution from the ligand-dependent route is immeasurable, since the rate constants observed for ligand substitution of III and IV are singularly invariant with the concentration of added trimethyl phosphite (Tables XI and XII). Coupled with the rather large positive entropy of activation measured under these circumstances (Table XIV), we propose a dissociative loss of CO as the rate-limiting step in ligand substitution, as depicted in Scheme II.[51] The subsequent steps are harder to pin down owing to the rapid rates of intramolecular carbonyl scrambling, which are several orders of magnitude faster than ligand substitution.[52] Thus the juncture at which the disposition of the phosphite ligands is determined cannot be established with certainty. For example, the tris-substituted cluster IV is formed with the phosphite ligands in an alternating syn/anti/syn configuration. It is likely that this stereochemistry results from a prior equilibrium of the bis(phosphite) III with 1,3-trans phosphites to the cis isomer in the coordinatively unsaturated intermediate formed by dissociative loss of CO. This rearrangement would then allow the entering

(45) (a) Wade, K. *Adv. Inorg. Chem. Radiochem.* **1976**, *18*, 1. (b) Wade, K. In *Transition Metal Clusters*; Johnson, B. F. G., Ed.; Wiley: New York, 1980; Chapter 3. (c) Mingos, D. M. P. *Adv. Organomet. Chem.* **1977**, *15*, 1. (d) For a discussion of the general bonding in these clusters, see: Halet, J. F.; Hoffman, R.; Saillard, J. Y. *Inorg. Chem.* **1985**, *24*, 1695.

(46) (a) Hieber, W.; Kruck, T. *Chem. Ber.* **1962**, *95*, 2027. (b) Bogan, L. E.; Lesch, D. A.; Rauchfuss, T. B. *J. Organomet. Chem.* **1983**, *250*, 429.

(47) For alteration of cluster polyhedra with capping ligands possessing large atomic radii, see: (a) Schmid, G. *Angew. Chem., Int. Ed. Engl.* **1978**, *17*, 392. (b) Efzrodt, G.; Schmid, G. *J. Organomet. Chem.* **1979**, *169*, 259. (c) Lesch, D. A.; Rauchfuss, T. B. *Inorg. Chem.* **1981**, *20*, 3583.

(48) Richmond, M. G.; Korp, J. D.; Kochi, J. K. *J. Chem. Soc., Chem. Commun.* **1985**, 1102.

(49) (a) Cf. the ligand substitution in $Ir_4(CO)_{12}$ in ref 39c. (b) See also: Bor, G.; Dietler, U. K.; Pino, P.; Poe, A. *J. Organomet. Chem.* **1978**, *154*, 301. (c) Fox, J. R.; Gladfelter, W. L.; Geoffroy, G. L. *Inorg. Chem.* **1980**, *19*, 2574. (d) Darensbourg, D. J.; Zalewski, D. J. *Inorg. Chem.* **1984**, *23*, 4382. (e) Muetterties, E. L.; Burch, R. R.; Stolzenberg, A. M. *Annu. Rev. Phys. Chem.* **1982**, *33*, 89.

(50) (a) Huttner, G.; Schneider, J.; Muller, H. D.; Mohr, G.; von Seyerl, J.; Wohlfahrt, L. *Angew. Chem., Int. Ed. Engl.* **1979**, *18*, 76. (b) Langenbach, H. J.; Keller, E.; Vahrenkamp, H. *Angew. Chem., Int. Ed. Engl.* **1977**, *16*, 188. (c) Carty, A. J.; MacLaughlin, S. A.; Taylor, N. J. *J. Organomet. Chem.* **1981**, *204*, C27. (d) Adams, R. D.; Yang, L. W. *J. Am. Chem. Soc.* **1983**, *105*, 235. (e) Richter, F.; Vahrenkamp, H. *Organometallics* **1982**, *1*, 756. (f) Field, J. S.; Haines, R. J.; Smit, D. N.; Natarajan, K.; Scheidsteger, O.; Huttner, G. *J. Organomet. Chem.* **1982**, *240*, C23.

(51) At this juncture we cannot state whether CO is lost at a substituted cobalt center or at an unsubstituted cobalt. The former process would be similar to the cis labilization effects observed by Atwood and Brown. For work relating to cis labilization in organometallic complexes, see: (a) Atwood, J. D.; Brown, T. L. *J. Am. Chem. Soc.* **1975**, *97*, 3380. (b) Atwood, J. D.; Brown, T. L. *J. Am. Chem. Soc.* **1976**, *98*, 3155. (c) Atwood, J. D.; Brown, T. L. *J. Am. Chem. Soc.* **1976**, *98*, 3160.

(52) Typically, the rates of CO scrambling at coalescence are estimated to be $10^3$–$10^4$ $s^{-1}$ for all compounds in this family.

phosphite access to the cluster and avoid any 1,2-cis interactions of phosphite ligands on contiguous cobalt centers. Alternatively, the observed tris-substituted cluster IV represents a thermodynamically equilibrated product.[53] Carbonyl fluxionality and steric effects within the cluster are expected to assist in directing the incoming phosphite to that site with the fewest unfavorable steric interactions.

The formation of the tetrakis(phosphite) V also represents a case in which a rearrangement of the phosphite ligands accompanies the ligand substitution of IV to V since we believe that the molecular structure in solution corresponds to that established by X-ray crystallography. The idealized $C_{2h}$ symmetry in V is reasonable if one considers the unfavorable steric interaction between a pair of 1,3-cis phosphite ligands and the $\mu_4$-phosphinidene cap (compare the bis(triphenylphosphine) derivative discussed above[36]).

Although the kinetics and activation parameters support a dissociative pathway in Scheme II for the ligand substitution of IV and V, the mechanistic analysis is not quite so straightforward for II and III. Thus, the magnitudes of the ligand-independent term ($k_1$) decrease more or less monotonically with increasing phosphite substitution on the cluster (see Table XIV). Such a trend in rate constants is indeed expected for a dissociative mechanism involving rate-limiting loss of CO.[54,55] However, the temperature dependence of the rate constant $k_1$ reveals a negative entropy of activation for the mono- and bis-substitutions, which is difficult to reconcile with a simple dissociative process.[56] It suggests the participation of a prior unimolecular reaction of the cluster—perhaps an opening of a carbonyl bridge or a scission of a non-carbonyl-bridged cobalt–cobalt bond—independent of CO loss or phosphite attack. We are further pressed to explain why the parent and the mono(phosphite) clusters would follow this pathway when the behavior of the bis- and tris(phosphite) is in accord with a more conventional dissociative mechanism in Scheme II. We expect the study of other types of ligands to provide the information needed to further delineate the role of electronic and steric effects of ligands on the chemistry of clusters.

## Summary and Conclusions

The ligand substitution of the tetracobalt $Co_4(CO)_{10}(\mu_4\text{-}PPh)_2$ (I) with excess trimethyl phosphite ultimately leads to a single tetrakis derivative, $Co_4(CO)_6[P(OMe)_3]_4(\mu_4\text{-}PPh)_2$ (V). By the judicious adjustment of the phosphite concentration and the temperature, the mono-, bis-, and tris(phosphites) II, III, and IV, respectively, can be isolated as intermediates and their molecular structures established by X-ray crystallography. The structures in Chart I show the stepwise substitution to occur at four separate cobalt centers in the following order: 1, 1, 3; 1, 3, 2; 1, 3, 2, 4. In each substitution product, the disposition of the entering phosphite is controlled by the steric interactions inherent in the cluster framework. The fluxional behavior of the carbonyl ligands allows the ready stereochemical interconversions of phosphite ligands as a particular tetracobalt cluster is converted to its next higher analogue.

The kinetics studies of $Co_4(CO)_{10}(PPh)_2$ reveal the presence of both phosphite-independent ($k_1$) and phosphite-dependent ($k_2$) terms for ligand substitution of the tetracobalt clusters. The magnitudes of $k_1$ and $k_2$ coupled with the measurement of the activation parameters indicate that the principal path for mono- and bis-substitution involves an associative mechanism in which phosphite attack on the cluster is rate-limiting. On the other hand, the kinetics of tris- and tetrakis-substitution are unaffected by added phosphite, which, together with the positive entropy of activation, reveals a dissociative process in which the loss of a CO ligand is rate-limiting. The changeover in mechanism as a result of increasing the extent of ligand substitution on the tetracobalt cluster[54,55] can be ascribed to the electronic effect of phosphites as electron donor ligands.[25] However, the unusual entropy of activation obtained for the minor kinetics term ($k_1$) in mono- and bis-substitution[56] suggests the presence of additional, more complex mechanisms for ligand substitution.

## Experimental Section

**Materials.** Dicobalt octacarbonyl and phenyldichlorophosphine (Pressure Chemical) were used as received. Trimethyl phosphite (Aldrich) was distilled twice from sodium and stored under argon. Toluene was distilled from sodium benzophenone and stored under argon. $Co_4(CO)_{12}$ was prepared according to the procedure of King.[57] The $^{13}C$-enriched carbon monoxide (99% $^{13}C$) was obtained from Mound Laboratory, Monsanto Research Corp.

**Synthesis of $Co_4(CO)_{10}(PPh)_2$.** To 50 mL of a toluene solution containing $NaCo(CO)_4$ (~0.006 mol) at −78 °C was added 0.4 mL (0.003 mol) of $PhPCl_2$. The reaction was stirred for 2.0 h at −78 °C and then allowed to warm to room temperature. The solution was filtered under argon using Schlenk techniques. The resulting solution was either refluxed for 2.0 h or stirred overnight at room temperature. (The yield of product was essentially the same by either procedure.) Solvent removal, followed by drying in vacuo, afforded a black residue, which was chromatographed on a silica gel column by eluting with hexane. The first band, which was golden yellow, corresponded to $Co_4(CO)_{10}(PPh)_2$. Typical yields of $Co_4(CO)_{10}(PPh)_2$ ranged from 15 to 30%. An analytically pure sample was obtained by crystallization from a 1:10 mixture of toluene and hexane at −20 °C. IR ($CH_2Cl_2$): $\nu_{CO}$ 2040 (vs), 2032 (s), 2016 (s), 1866 (w) $cm^{-1}$. UV ($CH_2Cl_2$): $\lambda_{max}$ 502 ($\epsilon$ 335), 428 (5705), 353 (15031), 307 nm (18975). Anal. Calcd for $C_{22}H_{10}Co_4O_{10}P_2$: C, 36.10; H, 1.38. Found: C, 35.60, H, 1.33.

**Synthesis of $Co_4(CO)_9[P(OMe)_3](PPh)_2$.** To 1.0 g (0.0014 mol) of $Co_4(CO)_{10}(PPh)_2$ in 100 mL of benzene was added 0.21 mL (0.0017 mol) of $P(OMe)_3$. The solution was stirred at 35 °C overnight and allowed to cool. TLC examination of the solution showed the major product to be the monosubstituted cluster II. The desired product was purified by chromatography on silica gel using an 8:2 (v/v) mixture of hexane and benzene. The resulting material was recrystallized from hexane at −20 °C to afford 0.79 g (62%) of red $Co_4(CO)_9[P(OMe)_3](PPh)_2$. IR ($CH_2Cl_2$): $\nu_{CO}$ 2058 (m), 2023 (vs), 2008 (s), 1850 (m) $cm^{-1}$. UV ($CH_2Cl_2$): $\lambda_{max}$ 432 ($\epsilon$ 7735), 358 (15466), 308 nm (17981).

**Synthesis of $Co_4(CO)_8[P(OMe)_3]_2(PPh)_2$.** To 1.0 g (0.0014 mol) of $Co_4(CO)_{10}(PPh)_2$ in 50 mL of benzene was added 0.4 mL (0.0032 mol) of $P(OMe)_3$. The reaction was stirred overnight at 45 °C. TLC examination of the reaction solution showed the major product to be that of the bis-substituted cluster. The desired product was purified by chromatography on silica gel using a 1:1 mixture of hexane and benzene. The resulting material was recrystallized from a 9:1 mixture of hexane and benzene at −20 °C to afford 0.67 g (55.8%) of red $Co_4(CO)_8[P(OMe)_3]_2(PPh)_2$. IR ($CH_2Cl_2$): $\nu_{CO}$ 2039 (m), 2008 (vs), 1985 (s), 1835 (m) $cm^{-1}$. UV ($CH_2Cl_2$): $\lambda_{max}$ 436 ($\epsilon$ 9292), 362 (14955), 309 nm (16766).

**Synthesis of $Co_4(CO)_7[P(OMe)_3]_3(PPh)_2$.** To 1.0 g (0.0014 mol) of $Co_4(CO)_{10}(PPh)_2$ in 50 mL of benzene was added 0.6 mL (0.0048 mol) of $P(OMe)_3$. The reaction mixture was refluxed for 6.0 h and then concentrated in vacuo to afford a red residue. Purification by chromatography with silica gel using benzene gave a red material free of other products, as shown by TLC. An analytically pure sample was recrystallized from a 1:10 mixture of toluene and hexane at −20 °C to yield 0.41 g (29% yield) of red $Co_4(CO)_7[P(OMe)_3]_3(PPh)_2$. IR ($CH_2Cl_2$): $\nu_{CO}$ 2020 (s), 1970 (vs), 1810 (m) $cm^{-1}$. UV ($CH_2Cl_2$): $\lambda_{max}$ 444 ($\epsilon$ 8348), 369 (12648), 318 nm (15529). Anal. Calcd for $C_{28}H_{27}Co_4P_5O_{16}$: C, 32.95; H, 3.63. Found: C, 32.90; H, 3.80.

**Synthesis of $Co_4(CO)_6[P(OMe)_3]_4(PPh)_2$.** To 0.68 g (0.00092 mol) of $Co_4(CO)_{10}(PPh)_2$ in 40 mL of benzene was added 0.5 mL (0.004 mol) of $P(OMe)_3$, and the solution was refluxed overnight. The tetrakis-substituted product was purified by silica gel chromatography using benzene as the eluant. An analytically pure sample was recrystallized

(53) In the tris- and tetrakis-substituted clusters, the solution and solid-state (KBr) IR spectra are quite similar. This suggests that the observed crystallographic structure is maintained in solution.

(54) Darensbourg, D. J.; Peterson, B. S.; Schmidt, R. E., Jr. *Organometallics* **1982**, *1*, 306.

(55) Cf. similar mechanistic changes in bis- and tris-substituted clusters described in ref 41 and see: (a) Darensbourg, D. J.; Baldwin-Zuschke, B. J. *Inorg. Chem.* **1981**, *20*, 3846. (b) Darensbourg, D. J.; Baldwin-Zuschke, B. J. *J. Am. Chem. Soc.* **1982**, *104*, 3906. (c) Sonnenberger, D. C.; Atwood, J. D. *Organometallics* **1982**, *1*, 694. (d) Atwood, J. D.; Wovkulich, M. J.; Sonnenberger, D. C. *Acc. Chem. Res.* **1983**, *16*, 350.

(56) However, we hasten to add that $k_1$ and $\Delta S^*$ for mono- and bis-substitution are both obtained from the extrapolation (i.e. intercepts) of experimental data. The value of $\Delta S^*$ is thus particularly subject to large errors, and the negative values must be confirmed by additional studies with other nucleophiles.

(57) King, R. B. *Organometallic Synthesis*; Academic: New York, 1965; Vol. 1.

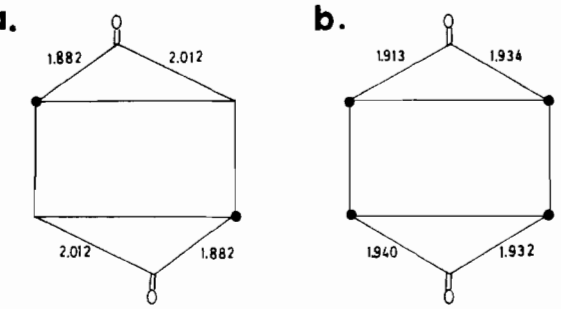


**Figure 7.** Comparison of the (bridging) CO–Co bond lengths (Å) in (a) $Co_4(CO)_8[P(OMe)_3]_2(PPh)_2$ and (b) $Co_4(CO)_6[P(OMe)_3]_4(PPh)_2$ by the projection across the tetracobalt plane. Closed circles indicate Co with the $P(OMe)_3$ ligand.

from a 1:1 mixture of toluene and hexane at −40 °C to yield 1.00 g (97%) of red $Co_4(CO)_6[P(OMe)_3]_4(PPh)_2$. IR ($CH_2Cl_2$): $\nu_{CO}$ 1985 (w), 1956 (vs), 1796 (m) $cm^{-1}$. UV ($CH_2Cl_2$): $\lambda_{max}$ 446 ($\epsilon$ 9968), 372 (13 132), 323 nm (16 964). Anal. Calcd for $C_{30}H_{46}Co_4O_{18}P_6$: C, 32.27; H, 4.12. Found: C, 32.16; H, 4.14.

**Instrumentation.** Infrared spectra were recorded in the linear absorbance mode on either a Perkin-Elmer 780 spectrophotometer or a Nicolet 10DX FT spectrometer in either 0.1- or 1.0-mm NaCl cells. Labline and Neslab RTE-3 constant-temperature baths were used to maintain the reactions at the desired temperatures to within ±0.1 °C. Variable-temperature $^{13}C$ NMR spectra were obtained at 75.5 MHz on a Nicolet 300 wide-bore spectrometer.

**X-ray Diffraction Study of $Co_4(CO)_8[P(OMe)_3]_2(PPh)_2$.** A large reddish black block of approximate dimensions 0.55 × 0.25 × 0.15 mm was mounted on a glass fiber in a random orientation on an Enraf-Nonius CAD-4 automatic diffractometer. The radiation used was Mo K$\alpha$ monochromatized by a dense graphite crystal assumed for all purposes to be 50% imperfect. Final cell constants, as well as other information pertinent to data collection and refinement, are listed in Table II. The Laue symmetry was determined to be $2/m$, and from the systematic absences noted the space group was shown unambiguously to be $P2_1/n$. Intensities were measured with use of the $\theta$–$2\theta$ scan technique, with the scan rate depending on the net count obtained in rapid prescans of each reflection. Two standard reflections were monitored periodically during the course of the data collection as a check of crystal stability and electronic reliability, and these did not vary significantly. Lorentz and polarization factors were applied in reducing the data; however, no correction for absorption was made.

The structure was solved by MULTAN,[58] which revealed the positions of the two Co and two P atoms in the asymmetric unit which comprises only a half-molecule situated about a center of inversion. The remaining non-hydrogen atoms were located in subsequent difference Fourier syntheses. One of the methyl groups (C5) is disordered over three positions, each having approximately one-third population. The usual sequence of isotropic and anisotropic refinement was followed, after which all hydrogens were entered in ideally calculated positions. In the final cycles of full-matrix least squares none of the hydrogen parameters were varied. Hydrogen isotropic temperature factors were estimated on the basis of the thermal motion of the associated carbons. After all shift/esd ratios were less than 0.1, convergence was reached at the agreement factors listed in Table III. No unusually high correlations were noted between any of the variables in the last cycle of least-squares refinement, and the final difference density map showed no peaks greater than 0.20 e/Å. All calculations were made by using Molecular Structure Corp.'s TEXRAY 230 modifications of the SDP-PLUS series of programs.

In $Co_4(CO)_8[P(OMe)_3]_2(PPh)_2$, the two $P(OMe)_3$ ligands are arranged in a 1,3-trans configuration with respect to the tetracobalt plane (i.e., they are related by inversion through the midpoint of the tetracobalt plane). The two carbonyl-bridged Co–Co bonds of 2.524 Å (av) are 0.19 Å shorter than the non-carbonyl-bridged Co–Co bonds of 2.713 Å (av). The terminal Co–CO distances range from 1.770 (4) to 1.788 (4) Å with a mean of 1.778 Å. The longer bridging Co–CO distances show the asymmetric coordination attendant upon substitution. Here the distances vary from 1.882 (4) to 2.012 (4) Å. Figure 7 shows the asymmetric bridging carbonyl in $Co_4(CO)_8[P(OMe)_3]_2(PPh)_2$ via a cross section through the tetracobalt plane. A similar observation of the shortening of the bridging OC–Co bond at a substituted cobalt center has also been noted in $Co_4(CO)_8(PPh_3)_2(PPh)_2$ and ascribed to an electronic effect derived from ligand substitution by a phosphorus-centered nucleophile.[36] The better $\sigma$-donating ability of the $P(OMe)_3$ ligand places greater electron density on the cobalt at the site of substitution relative to that at an unsubstituted site. This manifests itself in a greater degree of $\pi^*$ back-bonding and diminution of the length of the bridging Co–CO bond at the site of substitution. The lengths of the Co–P($\mu_4$) bonds of 2.245 Å (av) are in agreement with the bond lengths observed in the parent cluster $Co_4(CO)_{10}(PPh)_2$[16] and reinforce the symmetrical capping nature of the $\mu_4$-phenylphosphinidene moiety. In the bis-substituted cluster $Co_4(CO)_8(PPh_3)_2(PPh)_2$, the Co–P($\mu_4$) bond lengths were asymmetric. Here the phenyl substituents of the $PPh_3$ ligands experience greater intramolecular nonbonding repulsions with the phosphinidene phenyl groups. This results in a slight puckering of the tetracobalt plane with a concurrent lengthening of the Co–P($\mu_4$) bond at the site of $PPh_3$ substitution. In $Co_4(CO)_8[P(OMe)_3]_2(PPh)_2$, the smaller phosphorus ligand $P(OMe)_3$ shows no such steric interaction with the phosphinidene phenyls, as evidenced by the symmetrical coordination of the $\mu_4$-phosphinidene group and the absence of puckering in the tetracobalt plane.

**X-ray Diffraction Study of $Co_4(CO)_6[P(OMe)_3]_4(PPh)_2$.** A long, dark purple, square column of approximate dimensions 0.50 × 0.15 × 0.15 mm was mounted on the diffractometer (vide supra). Final cell constants, as well as other information pertinent to data collection and refinement, are listed in Table II. The Laue symmetry was determined to be 1, and the space group was shown to be either $P1$ or $P\bar{1}$. Intensities were measured with use of the $\theta$–$2\theta$ scan technique, with the scan rate depending on the net count obtained in rapid prescans of each reflection. Two standard reflections were monitored periodically during the course of the data collection as a check of crystal stability and electronic reliability, and these did not vary significantly. In reduction of the data, Lorentz and polarization factors were applied, as well as an empirical absorption correction based on azimuthal $\psi$ scans of six reflections having $\chi$ near 90°.[59]

The structure was solved by use of MULTAN,[58] which revealed the positions of four cobalt and five phosphorus atoms in the asymmetric unit. This unit was found to consist of two half-molecules, each situated about a different center of inversion. The usual sequence of isotropic and anisotropic refinement was followed, after which all hydrogens were entered in ideally calculated positions and held fixed. After all shift/esd ratios were less than 0.1, the full-matrix least squares converged at the agreement factors listed in Table IV. Anomalous dispersion coefficients for the heavier elements were included. No unusually high correlations were noted between any of the variables in the last cycle of least-squares refinement, and the final difference density map was featureless. All calculations were made as noted above.

$Co_4(CO)_6[P(OMe)_3]_4(PPh)_2$ is the first reported example of a tetrakis-substituted phosphite cluster of this general structure type. The disposition of the $P(OMe)_3$ groups as elucidated by X-ray diffraction in the idealized $C_{2h}$ symmetry inherent in this cluster is readily seen from Figure 2b. The $P(OMe)_3$ groups on Co1 and Co2 are bound in a 1,2-cis manner and are related to the 1′,2′-cis-$P(OMe)_3$ groups by inversion through the midpoint of the tetracobalt plane. Overall, the 1,2-cis-$P(OMe)_3$ groups of $Co_4(CO)_6[P(OMe)_3]_4(PPh)_2$ closely parallel those in $Co_4(CO)_8[P(OMe)_3]_2(PPh)_2$. For example, the two carbonyl-bridged Co–Co bond lengths are 2.520 Å (av) and the non-carbonyl-bridged Co–Co bond lengths are 2.727 Å (av). The four terminal Co–CO distances possess a mean of 1.769 Å (av), and the Co–P($\mu_4$) distances range from 2.246 (9) to 2.259 (9) Å with 2.253 Å (av) as the mean distance. The capping phosphinidene is symmetrically bound to the tetracobalt core as in $Co_4(CO)_8[P(OMe)_3]_2(PPh)_2$ and $Co_4(CO)_{10}(PPh)_2$.[16] The bridging carbonyls are found to be symmetrically bound with Co–CO distances ranging from 1.913 (8) to 1.940 (8) Å and 1.930 Å representing the average. This is illustrated in Figure 7, showing the direct comparison with $Co_4(CO)_8[P(OMe)_3]_2(PPh)_2$. As expected, the substitution of $P(OMe)_3$ at each cobalt removes the asymmetry that is observed in the less substituted derivatives. The lengthening of the Co–CO bridging carbonyl distances (1.930 Å) is readily seen when they are compared to those in the unsubstituted $Co_4(CO)_{10}(PPh)_2$, in which the Co–CO bridging bonds are 1.89 Å. The better $\sigma$-donating properties of $P(OMe)_3$ are responsible for this bond elongation. The cis arrangement of the $P(OMe)_3$ ligands across the carbonyl-bridged Co–Co bond produces slight perturbations on the molecular structure of the cluster. The bridging carbonyls are pushed slightly out of the tetracobalt plane (~ 3.5°) away from the $P(OMe)_3$ groups, and the phenyl groups of the phosphinidene capping ligands are tilted away from the cis-$P(OMe)_3$ groups and toward the opposite terminal carbonyls by approximately 4° relative to the positions in $Co_4(CO)_{10}(PPh)_2$.[16] Finally, the tetracobalt framework experiences no extenuating steric interactions as evidenced

(58) Germain, G.; Main, P.; Woolfson, M. M. *Acta Crystallogr., Sect. A: Cryst. Phys., Diffr., Theor. Gen. Crystallogr.* **1971**, *A27*, 368.

(59) North, A. C. T.; Phillips, D. C.; Matthews, F. S. *Acta Crystallogr, Sect. A: Cryst. Phys., Diffr., Theor. Gen. Crystallogr.* **1968**, *A24*, 351.

by the absence of puckering in the tetracobalt plane.

**Isotopic Enrichment of Tetracobalt Clusters. $^{13}CO$ Enrichment of $Co_4(CO)_{10}(PPh)_2$.** Direct reaction of $^{13}CO$ with $Co_4(CO)_{10}(PPh)_2$ in benzene at temperatures up to 50 °C afforded the $^{13}CO$-enriched cluster to only a small extent (~5%). Similar results were obtained using photochemical procedures. The synthesis of $^{13}CO$-enriched $Co_4(CO)_{10}(PPh)_2$ was accomplished from $Co_4(CO)_{12}$ as the starting material in the following way. $Co_4(CO)_{12}$ was enriched in $^{13}CO$ by repeated exposure to an atmosphere of $^{13}CO$. The $^{13}CO$-enriched $Co_4(CO)_{12}$ (2.4 g, 0.42 mmol, with 40% $^{13}CO$) was reduced with sodium amalgam in THF under an atmosphere of $^{13}CO$ to afford the tetracarbonylcobaltate. The solution of $Co(CO)_4^-$ was filtered over Celite and used immediately in the next step. To the filtrate was added 1.2 mL (0.0084 mol) of $PhPCl_2$ in 40 mL of THF. The reaction was stirred for 24 h at room temperature and worked up as previously described for $Co_4(CO)_{10}(PPh)_2$. The IR spectrum indicated the resulting product to be ~40% $^{13}CO$ enriched; yield 1.5 g (~50% based on $PhPCl_2$).

**$^{13}CO$ Enrichment of $Co_4(CO)_9[P(OMe)_3](PPh)_2$.** $Co_4(CO)_9[P(OMe)_3](PPh)_2$ (0.15 g, 0.18 mmol) in 10 mL of toluene under 0.9 atm of $^{13}CO$ was irradiated at 355 nm (Rayonet Photochemical Reactor) for 1 week at room temperature. The cluster was recovered in essentially quantitative yield after purification by chromatography. It was found to be ~15% $^{13}CO$ enriched, as judged by its IR spectrum.

**$^{13}CO$-Enriched $Co_4(CO)_8[P(OMe)_3]_2(PPh)_2$.** $Co_4(CO)_{10}(PPh)_2$ (0.10 g, 0.14 mmol of $^{13}CO$-enriched sample) in 7 mL of THF containing 0.1 M TBAP was electrolyzed in a bulk electrolysis cell at constant current (-1.2 V) until the conversion to the bis-substituted cluster III was complete, as observed by TLC. This procedure has already been shown to afford selectively and catalytically the bis-substituted cluster.[15] The product was isolated by column chromatography and recrystallized from hexane. The bis(phosphite) was judged to be ~40% $^{13}CO$ enriched by IR spectroscopy; yield 0.09 g (~71%).

**$^{13}CO$-Enriched $Co_4(CO)_7[P(OMe)_3]_3(PPh)_2$.** $Co_4(CO)_6[P(OMe)_3]_4$ (0.14 g, 0.14 mmol, of ~40% $^{13}CO$-enriched complex, vide infra) in 10 mL of toluene was stirred at room temperature for 1 week under 1 atm of $^{13}CO$. At that time, the quantitative conversion to the tris-substituted cluster IV was observed and the product was judged to contain ~40% $^{13}CO$ by IR spectroscopy.

**$^{13}CO$-Enriched $Co_4(CO)_6[(OMe)_3]_4(PPh)_2$.** To $Co_4(CO)_{10}(PPh)_2$ (0.1 g, 0.14 mmol, of ~40% $^{13}CO$-enriched sample) in 20 mL of toluene was added 0.2 mL (excess) of $P(OMe)_3$. The reaction was heated at ~70 °C overnight and then allowed to cool. TLC examination revealed only the tetrakis-substitution product V to be present. The product was isolated by chromatography and found to be ~40% $^{13}CO$ enriched by IR spectrophotometry; yield 0.14 g (~90%).

**Kinetics Studies.** All kinetics runs were performed under pseudo-first-order conditions, with $P(OMe)_3$ concentrations which were greater than 10 times that of the reactant cluster. The reactions were all monitored for a minimum of 3 half-lives by following the IR absorbance of the highest energy band of the starting cluster. Plots of ln $A_T$ vs. time afforded the pseudo-first-order rate constants, $k_{obsd}$, listed in Tables VII and IX. In the kinetics studies of $Co_4(CO)_{10}(PPh)_2$ and $Co_4(CO)_9[P(OMe)_3](PPh)_2$ the plots of $k_{obsd}$ vs. the $P(OMe)_3$ concentration afforded the ligand-independent and -dependent rate constants, $k_1$ and $k_2$, respectively. The activation parameters ($\Delta H^{\ddagger}$ and $\Delta S^{\ddagger}$) were determined from the usual plots of the temperature dependences of $k_1$ and $k_2$. Error limits were calculated by using the available least-squares regression program.[60]

The energies of activation in Table XIII were calculated according to the procedure given by Shanan-Atidi and Bar-Eli.[31] Here the bridging carbonyls and terminal carbonyls were treated as unequal doublets capable of undergoing intramolecular exchange. The relative populations of the carbonyls were obtained from the integration of the slow-exchange spectrum. A variable-temperature $^{13}C$ NMR study allowed the determination of $T_c$, the coalescence temperature. At this temperature the observed chemical shift was found to be in good agreement with the weighted-average chemical shifts obtained from the slow-exchange spectrum. We have assumed that this behavior represents complete, intramolecular carbonyl scrambling about the cluster polyhedron. Through the use of the relative populations of exchanging carbonyls and the coalescence temperature, the activation energy for intramolecular carbonyl scrambling was calculated with the aid of the modified Eyring equation.[61]

**Acknowledgment.** We thank Dr. James D. Korp for the crystal structures in Figure 2 and the National Science Foundation and the Robert A. Welch Foundation for financial support.

**Registry No.** I, 58092-22-1; II, 86372-99-8; III, 100190-64-5; IV, 99918-23-7; V, 99918-24-8; $P(OMe)_3$, 121-45-9; $NaCo(CO)_4$, 14878-28-5; $PhPCl_2$, 644-97-3.

**Supplementary Material Available:** Lists of the bond lengths and angles of the methoxy and phenyl groups and structure factor amplitudes (21 pages). Ordering information is given on any current masthead page.

(60) Gordon, A. J.; Ford, R. A. *The Chemist's Companion: A Handbook of Practical Data, Techniques, and References*; Wiley: New York, 1976.
(61) Glasstone, S.; Laidler, K. J.; Eyring, H. *The Theory of Rate Processes*; McGraw-Hill: New York, 1941.

---

Contribution from the Science Research Laboratory, 3M Central Research Laboratories, St. Paul, Minnesota 55144, and Department of Chemistry, University of Minnesota, Minneapolis, Minnesota 55455

# Organometallic Chemistry of Fluorocarbon Acids. Synthesis, Structure, and Solvolysis of a Sulfinate-Bridged Diruthenium Dihydride Cluster, $[(Ph_3P)_4Ru_2(\mu\text{-}H)_2(\mu\text{-}CF_3SO_2)(CO)_2]HC(SO_2CF_3)_2$

A. R. Siedle,*† R. A. Newmark,† and L. H. Pignolet‡

*Received October 16, 1985*

Reaction of $(Ph_3P)_3RuH_2(CO)$ with 2 equiv of the fluorocarbon acids $H_2C(SO_2CF_3)_2$ or $PhCH(SO_2CF_3)_2$ in toluene at >80 °C produces the $HC(SO_2CF_3)_2^-$ or $PhC(SO_2CF_3)_2^-$ salts of $(Ph_3P)_4Ru_2(\mu\text{-}H)_2(\mu\text{-}CF_3SO_2)(CO)_2^+$, in which the bridging hydrides were located by very high field $^1H$ NMR. The bridging bidentate $CF_3SO_2$ group in $[(Ph_3P)_4Ru_2(\mu\text{-}H)(\mu\text{-}CF_3SO_2)(CO)_2]HC(SO_2CF_3)_2\cdot CH_2Cl_2$ was established by single-crystal X-ray diffraction [$P\bar{1}$ (triclinic), $a$ = 16.300 (3) Å, $b$ = 17.783 (4) Å, $c$ = 14.496 (2) Å, $\alpha$ = 92.74 (1)°, $\beta$ = 90.84 (1)°, $\gamma$ = 111.82 (1)°, $Z$ = 2]. This compound reacts with acetonitrile to form salts of $(Ph_3P)_2RuH(CO)(CH_3CN)_2^+$. In the $HC(SO_2CF_3)_2^-$ derivative [$P2_1/n$ (monoclinic), $a$ = 14.561 (3) Å, $b$ = 16.858 (3) Å, $c$ = 19.122 (4) Å, $\beta$ = 93.55 (2)°, $Z$ = 4], $d$(Ru-N, trans to CO) is 2.108 (5) Å while $d$(Ru-N, trans to H) is 2.163 (5) Å and one of the acetonitrile ligands rapidly exchanges with $CD_3CN$.

## Introduction

We have previously described the organometallic chemistry of the novel fluorochemical acids **1** and **2**[1] and showed how these compounds can be used in the absence of donor solvents to synthesize cationic metal hydrides that contain the noncoordinating counterions $HC(SO_2CF_3)_2^-$ and $PhC(SO_2CF_3)_2^-$.[2,3] High

† 3M Central Research Laboratories.
‡ University of Minnesota.

(1) Koshar, R. J.; Mitsch, R. A. *J. Org. Chem.* **1973**, *38*, 3358.
(2) Siedle, A. R.; Newmark, R. A.; Pignolet, L. H.; Howells, R. D. *J. Am. Chem. Soc.* **1984**, *106*, 1510.

0020-1669/86/1325-1345$01.50/0 